UNIVERSITÀ DEGLI STUDI DI GENOVA

DEPARTMENT OF INTERNAL MEDICINE

CLINICAL AND EXPERIMENTAL IMMUNOLOGY SCHOOL

PhD THESIS

Investigating the Effects of TREM2 Modulation with *In-Vitro* Models & Profiling the Proteome of Alzheimer's Disease (and other Neurological Diseases) Cerebrospinal Fluid

SUPERVISORS:
Prof. Gilberto Filaci, PhD
Heather Cooke, PhD
John Silbereis, PhD
Chia-Chen (Jenny) Liu, PhD

CANDIDATE:
Danté Duncan
Matr. S5515545

2025/2026

Table of Contents

Introduction (Section 1)

Alzheimer's Disease (AD) is the most common form of dementia and most common neurodegenerative disease, accounting for 60-80% of all dementia cases[1]. As of 2020, 55 million people worldwide were living with dementia[2], while more recently in 2024, it was estimated that 6.9 million people were living with AD in the United States[3]. AD is a progressive neurodegenerative disease, and is most often characterized by two main pathologies, extracellular β-amyloid plaques (Aβ) and intracellular neurofibrillary tangles (NFTs) of hyperphosphorylated tau protein. The accumulation of Aβ plaques and NFTs leads to neuronal dysfunction, progressive brain atrophy, and ultimately results in cognitive decline[4, 5]. Presently, there are only two approved therapies for the treatment of AD, both of which target Aβ pathology, and though efficacy has been demonstrated, the extent of the benefits from these treatments are still debated[6, 7]. Many clinical trials targeting the removal of Aβ plaques and NFTs have failed, although there are currently active trials targeting tau protein, which leads to NFTs, that may prove beneficial in slowing the progression of AD.

Recent advancements have demonstrated numerous other underlying factors that contribute to the development of AD, but in particular, one area that has generated large interest is neuroinflammation[8]. In fact, neuroinflammation is now seen by some as a key driver of AD progression, as opposed to being a consequence of the disease[9]. Different studies have suggested that the development and subsequent progression of AD is directly associated with chronic inflammation in the central nervous system (CNS)[9]. In the CNS, both microglia and astrocytes are key cells involved in the inflammatory state and they play an essential role in maintaining homeostasis. Microglia are the resident immune cells of the CNS. Microglia comprise 5-10% of the total cell population within the central nervous system[10]. Microglia have numerous critical functions, including phagocytosis of apoptotic cells during brain development, myelin turnover, phagocytosis of debris, synaptic pruning and generally, are responsible for responding and protecting the brain from injury[11].

Interestingly, of all the genes associated with increased risk of developing sporadic Alzheimer's disease, which is by far the most common form of AD, nearly half of these genes are more highly expressed by microglia than any other cell type in the brain[12, 13]. These findings demonstrate how microglial dysfunction can drive disease progression. Among the many genes implicated with increased risk of sporadic AD, triggering receptor on myeloid cells 2 (TREM2) is the second most strongly associated gene with AD risk[14, 15], behind only the ϵ4 allele of Apolipoprotein E (APOE), APOE-ϵ4[16, 17]. The most common TREM2 mutation is the R47H loss-of-function mutation, and is associated with a 2-3 fold higher risk of developing sporadic AD[14]. TREM2 is highly specific to microglia within the CNS, and is involved in numerous microglial functions, including phagocytosis, chemotaxis, survival, cytokine and chemokine secretion, and activation state[18-20]. TREM2 is a transmembrane receptor protein, consisting of an extracellular Ig-like V-type domain (IgV), a short ectodomain, a single transmembrane helix and a small cytosolic tail that does not directly induce any downstream signaling[19, 21]. Instead, signal transduction occurs when TREM2 associates with the adaptor proteins DNAX activation protein 12 (DAP12) and DAP10, causing the phosphorylation and activation of spleen tyrosine kinase Syk (pSyk) and recruitment of phosphatidylinositol 3-kinase (PI3K), which in turn results in further downstream signaling[19]. Numerous ligands have previously been shown to bind TREM2 and activate the TREM2 (and DAP10/12) signaling pathway, including large anionic molecules, β-amyloid, apoliproteins, phospholipids, as well as bacterial and mammalian cells[19, 21-26].

Previous studies have shown that TREM2 loss of function or knockout (KO) mutations significantly impair various microglial functions, impacting phagocytosis, energy metabolism, migration, proliferation, inflammatory response and Aβ plaque compaction[24, 27-29]. Interestingly, studies investigating TREM2 using *in-vitro* models and *in-vivo* AD models have shown conflicting results. One *in-vitro* study found that the TREM2 R47H mutation did not impact the TREM2 signaling cascade, or reduce key cellular functions, like phagocytosis and survival, whereas a TREM2 KO cell line experienced reduced

signaling and function[18]. An *in-vivo* study using a prominent AD mouse model, 5XFAD, found that TREM2 deficiency worsened Aβ plaque burden and blunted microglial viability, while the R47H mutation only reduced the ability of TREM2 to bind lipid ligands[30]. Another *in-vivo* study, using a different AD mouse model, APPPS1, found that the mice lacking TREM2 had reduced Aβ deposits and less neuroinflammation[31]. In summary, while it is clear that loss of function TREM2 mutations are directly associated with increased risk of AD, the exact mechanisms that increase this risk are still being debated.

Microglia are highly active cells and can rapidly change their state to adjust to their environment[32]. It has been suggested that overactivation of microglia results in them becoming "exhausted", where they can no longer respond to injury or disease phenotypes[33]. As Alzheimer's disease progresses, there is likely a continuum, where microglia originally play a neuroprotective role, but as disease burden becomes too great, microglia begin to have a neurotoxic role and advance the disease[25, 34].

The genetic association of TREM2 and AD has led to significant research around the therapeutic potential of TREM2, with many companies actively developing drug candidates targeting TREM2 in AD, and other related neurodegenerative diseases[35-37]. Unfortunately, clinical trial assessments of investigational TREM2 targeting therapies have not reached their primary endpoints, and further development has been discontinued[38]. Even with some setbacks, the field appears to remain committed to targeting TREM2. For example, Vigil Neuroscience was acquired by Sanofi in 2025, and its TREM2 targeting small molecule will remain in development[39]. Another small company, Muna Therapeutics, is developing a TREM2 small molecule agonist and is currently studying its safety in a Phase 1 study.

Previous preclinical studies have shown that therapeutically relevant TREM2 targeting molecules, mainly monoclonal antibodies, have an ability to rescue TREM2 LOF mutations or improve phenotypes in AD models[40-42]. In this work, we aim to understand if anti-TREM2 monoclonal

antibodies with differing mechanisms of action have unique downstream effects using two separate *in-vitro* models. We investigate if the type of TREM2 activation impacts microglial viability, neuroinflammation (as a result of cytokine and chemokine secretion), as well as microglial migration.

Study Aims (Section 2)

Study Aim #1 (2.1)

There still exists heightened interest in TREM2 as a possible therapeutic target for treating Alzheimer's disease (AD) and other neurodegenerative diseases, despite recent clinical failures. Of note, there are conflicting data regarding the biologic and mechanistic impacts TREM2 plays in AD progression. We aim to further understand how microglial function is differentially impacted by unique methods of TREM2 modulation with monoclonal anti-TREM2 antibodies. This study will focus on three different functions of microglia, all of which are associated with TREM2 signaling, including cytokine and chemokine secretion, viability and migration[18-20]. The two main TREM2 targeting antibodies that will be used in this study are internally generated and mimic two antibodies that were being investigated in AD or other neurodegenerative diseases, specifically the TREM2 antibody developed by Alector and the TREM2 antibody developed by Vigil (now Sanofi). *Note: while these are mimic antibodies, the antibodies will simply be referred to as the Alector antibody or the Vigil antibody, hereafter, for simplicity.*

Two *in vitro* models, THP1 cells (differentiated into macrophages) and induced pluripotent stem cell (iPSC) induced microglia-like cells (iMGLs), were used to assess the impacts of TREM2 modulation on microglial function. THP1s were initially selected as they have been extensively used to study monocyte or macrophage function, and these cells constitutively express TREM2[43]. To better understand how TREM2 modulation impacts microglial-specific function, the more biologically relevant iMGL model was used.

As previously mentioned, in this work, we aim to understand if anti-TREM2 monoclonal antibodies have differing downstream effects using two separate in-vitro models. We investigate if the type of TREM2 activation impacts microglial viability, neuroinflammation (as a result of cytokine and chemokine secretion), as well as microglial migration.

Study Aim #2 (2.2)

As newer, ultra-sensitive technologies are developed, there are evolving efforts to more thoroughly profile the cerebrospinal fluid (CSF) of individuals with Alzheimer's disease (AD), and other neurological diseases. For many of these diseases, particularly AD, the field is also looking to transition biomarkers (CSF and blood) from merely research tools to measurements with clinical usefulness[44, 45]. One recent study shows the benefit of a sensitive technology from both perspectives, whereby the researchers profiled CSF from AD patients and identified five molecular subtypes, each with a unique genetic risk profile for developing AD[46]. These kinds of studies are especially useful given the heterogeneous nature of AD, and ultimately, findings that help differentiate AD may provide insight on what therapies are best for certain patients.

We aim to identify CSF biomarkers that could prove beneficial from a research prospective, and also be considered for further evaluation as exploratory biomarkers in AD, with clinically relevant endpoints in mind. We plan to identify proteins that are differentially expressed in AD CSF, compared to other neurological diseases, specifically looking if any differentially expressed proteins are relevant to microglial function. We will test untreated CSF samples from multiple clinical studies investigating various neurological diseases, including Alzheimer's disease, Parkinson's disease (PD), amyotrophic lateral sclerosis (ALS) and progressive supranuclear palsy (PSP). By profiling these CSF samples using an innovative, ultra-sensitive technology, called O-link®, we hope to identify unique protein signatures in AD CSF, when compared to these other neurological diseases. Through this, we aim to identify biomarkers that could be further explored from a research perspective (possible relation to AD pathology), or for potential use as a biomarker with clinical utility.

Methods (Section 3)

THP1 Cell Culture (3.1)

THP1 cells (ATCC #TIB-202) were cultured in a maintenance media, containing: 1X RPMI Medium 1640 (Gibco #21870076), 10% fetal bovine serum (FBS) (Gibco #A5670201), 1X GlutaMax (Gibco #35050061), 1X Pen-Strep (Gibco 15140122), 10 mM HEPES Buffer Solution (Gibco #15630106), 1 mM Sodium Pyruvate (Gibco 11360070), 2-Mercaptoethanol (3.5 µL/L) (Gibco 21985023). THP1 cells were maintained at approximately $0.3x10^6$ cells/mL in T175 flasks in a 37°C incubator (5% carbon dioxide), with media replacements occurring every 3-4 days.

THP1 Differentiation (3.2)

100,000 THP1 cells were seeded per well in 96-well flat bottom cell culture plates (Costar #3595) and differentiated in 100 µL THP1 maintenance media that included 50 nM PMA (Sigma #P8139). The THP1 cells were incubated for 48 hours in a 37°C incubator (5% carbon dioxide). Prior to subsequent assays, the differentiated THP1s (THP1-derived macrophages) underwent an overnight media exchange into starvation media (serum free THP1 media).

Differentiated THP1 Supernatants – MSD IP-10 V-PLEX Assay (3.3)

Following the overnight serum starvation, the differentiated THP1s were treated with anti-TREM2 antibodies in 100 µL maintenance or starvation media (in quadruplicates) for 24 hours. Following the incubation, the supernatants were prepared for the MSD IP-10 V-PLEX assay (#K151NVD-2). The supernatants were diluted 4X in Diluent 43. The kit provided calibrators were prepared as instructed (7 non-zero calibrators and 1 blank, or diluent only). The MSD plate was washed 3X, then 50 µL of calibrators and diluted samples were added to the corresponding wells, in duplicates, and incubated for 2 hours at room temperature (shaking at 700 rpm). The plate was washed 3X, then 25 µL of IP-10 detection antibody solution was added to each, and incubated for 2 hours at room temperature (shaking

at 700 rpm). The plate was washed 3X, then 150 µL of 2X MSD Read Buffer T was added to each well, and incubated at room temperature for 10 minutes. The plate was read using a MSD plate reader. All analysis was performed in SoftMax Pro and GraphPad Prism.

Differentiated THP1 Lysates – CellTiter-Glo® Assay (3.4)

Following the overnight serum starvation, the differentiated THP1s were treated with anti-TREM2 antibodies in 100 µL maintenance or starvation media (in quadruplicates) for 24 hours. Following the incubation, supernatant was removed for separate analyses. The remaining cells were lysed with 100 µL CellTiter-Glo® substrate (Promega #G7572) for 2 minutes at 500 rpm using an orbital shaker. The cells were then incubated at room temperature for 10 minutes. The resulting cell lysates were transferred to a new 96-well flat white bottom cell culture plate (ThermoFisher #136101). The plate was read using a SpectraMax plate reader with luminescence capabilities. All analysis was performed in SoftMax Pro and GraphPad Prism.

iMGL Maturation (3.5)

A detailed protocol about generating human induced pluripotent stem cell (iPSC) induced microglia-like cells (iMGLs) has been described previously[47]. Briefly, 20,000-50,000 premature iPSC-derived microglia-like cells were seeded per well in 96-well flat bottom tissue culture plates (Costar #3595) and matured for 7 days in 200 µL iMGL maturation media. Maturation media was comprised of: Advanced DMEM/F12 (Gibco #12634028), 1X PenStrep (Gibco #15140122), 1X GlutaMax (Gibco #35050061), 1X N2 Supplement (Gibco #17502048), 55 µM β-Mercaptoethanol (BME) (Gibco #21985023), 10 ng/mL GM-CSF (StemCell Technologies #78190) and 100 ng/mL IL-34 (Peprotech #200-34). Over the 7 day maturation period, media was replaced every 2 or 3 days.

iMGL CellTiter-Glo® Assay (3.6)

50,000 iPSC-derived microglia-like cells were seeded per well in 96-well flat bottom tissue culture plates and matured for 7 days in 200 µL iMGL maturation media. Maturation media was comprised of: Advanced DMEM/F12, 1X PenStrep, 1X GlutaMax, 1X N2 Supplement, 55 µM BME, 10 ng/mL GM-CSF and 100 ng/mL IL-34. Over the 7 day maturation, media was replaced every 2 or 3 days. Upon completion of iMGL maturation, the maturation media was replaced with 200 µL maturation media and corresponding antibody was added at varying final concentrations. 5 biological replicates were included for each condition. The iMGLs were incubated for 72 hours, then supernatants were frozen for future chemokine analysis. The viability of the iMGLs was measured with the CellTiter-Glo® assay (Promega #G7571). Assay reagents were thawed and equilibrated to room temperature. The CellTiter-Glo® Substrate was then reconstituted with 10 mL of CellTiter-Glo® Buffer, forming the CellTiter-Glo® Reagent. 200 µL of CellTiter-Glo® Reagent was added to the iMGLs, and the contents were mixed for 2 minutes on an orbital shaker to induce cell lysis. The contents were incubated at room temperature for 10 minutes. The contents were then transferred to a 96-well flat white bottom tissue culture plate (ThermoFisher #136101). Luminescence was read on a SpectraMax plate reader. All analysis was performed in GraphPad Prism.

iMGL Multiplexed CellTiter-Fluor™ & Caspase-Glo® 3/7 Assay (3.7)

50,000 iPSC-derived microglia-like cells were seeded per well in 96-well flat bottom tissue culture plates and matured for 7 days in 200 µL iMGL maturation media. Maturation media was comprised of: Advanced DMEM/F12, 1X PenStrep, 1X GlutaMax, 1X N2 Supplement, 55 µM BME, 10 ng/mL GM-CSF and 100 ng/mL IL-34. Over the 7 day maturation, media was replaced every 2 or 3 days. Upon completion of iMGL maturation, the maturation media was replaced with 200 µL maturation media and corresponding antibody was added at 1 nM or 100 nM final concentration. 6 biological replicates were included for each condition. Viability of the iMGLs was measured with the CellTiter-Fluor™ assay

(Promega #G6080) and apoptotic iMGLs were measured with the Caspase-Glo® 3/7 assay (Promega #G8090). Assay reagents were thawed and equilibrated to room temperature. The GF-AFC substrate was briefly vortexed and centrifuged, then 10 µL GF-AFC substrate was added 2 mL assay buffer. The Caspase Buffer was transferred into the bottle containing Caspase Substrate, and gently mixed. Following the iMGL incubation, 100 µL supernatant was transferred to a new 96-well flat bottom tissue culture plate. In the original plate (containing the iMGLs), 20 µL CellTiter-Fluor™ reagent (GF-AFC in assay buffer) was added to each well, and the plate was briefly mixed using an orbital shaker. The resulting mixture was incubated for 1 hour at 37°C, then fluorescence was measured using a Promega reader. Subsequently, 120 µL of Caspase-Glo® 3/7 reagent was added to each well. The resulting mixture was incubated for 1 hour at room temperature in the dark, then luminescence was measured using a Promega reader. All analysis was performed in GraphPad Prism.

iMGL Supernatants – MSD V-PLEX Human Chemokine Panel 1 Gen. B Assay (3.8)

50,000 iPSC-derived microglia-like cells were seeded per well in 96 well flat bottom tissue culture plates and matured for 7 days in 200 µL iMGL maturation media. Maturation media was comprised of: Advanced DMEM/F12, 1X PenStrep, 1X GlutaMax, 1X N2 Supplement, 55 µM BME, 10 ng/mL GM-CSF and 100 ng/mL IL-34. Over the 7 day maturation, media was replaced every 2 or 3 days. Upon completion of iMGL maturation, the maturation media was replaced with 200 µL maturation media and corresponding antibody was added at varying final concentrations. 5 biological replicates were included for each condition. The iMGLs were incubated for 72 hours, then supernatants were frozen for future chemokine analysis using the MSD V-PLEX Human Chemokine Panel 1 Gen. B assay (Cat # K15705D-2). Briefly, supernatants were thawed and diluted 8X in MSD Diluent 57. The kit provided calibrators were prepared as instructed (7 non-zero calibrators and 1 blank, or diluent only). The plate was washed 3X, then 50 µL of calibrators and diluted samples were added to the plate, in duplicates, and incubated for 2 hours at room temperature (shaking at 700 rpm). The plate was washed 3X, then 25 µL of detection

antibody solution (containing 9 kit provided antibodies), was added to the plate, and incubated for 2 hours at room temperature (shaking at 700 rpm). The plate was washed 3X, and 150 µL of MSD Gold Read Buffer B was added to each well. The plate was read using a MSD plate reader. All analysis was performed in SoftMax Pro and GraphPad Prism.

iMGL Transwell Assay (3.9)

50,000 iPSC-derived microglia-like cells were seeded per 8.0 µm pore size transwell membrane (Fisher #3422) in 24-well flat bottom tissue culture plates (included with the transwell membranes). The iMGLs were seeded in 200 µL iMGL maturation media in the upper compartment. Additionally, 600 µL iMGL maturation media was added to the lower compartment. The cells were matured for 7 days. Maturation media was comprised of: Advanced DMEM/F12, 1X PenStrep, 1X GlutaMax, 1X N2 Supplement, 55 µM BME, 10 ng/mL GM-CSF and 100 ng/mL IL-34. Over the 7 day maturation, media was replaced every 2 or 3 days. Upon completion of iMGL maturation, the maturation media was replaced with 200 µL starved media (lacking GM-CSF and IL-34) in the upper compartment. The bottom compartment was replaced with 600 µL complete maturation media, 1 µM or 5 µM Aβ1-42 fibrils (AnaSpec #AS-20276), or 30 nM C5a (ThermoFisher #300-70-100UG). 6 biological replicates were included for each condition. The iMGLs were allowed to migrate for 48 hours. Then, the iMGLs were fixed with 10% neutral buffered formalin (NBF) (Epredia Signature Series #22-046329) for 30 minutes at room temperature, and stained with 1 µg/mL Hoechst (ThermoFisher #62249) for 10 minutes at room temperature in the dark. The transwell membrane inserts were transferred to a fresh 24-well flat bottom tissue culture plate, with 200 µL 1X Dulbecco's Phosphate Buffered Saline (DPBS) (Corning #21-031-CV) in the upper compartment and 600 µL 1X DPBS in the lower compartment. The iMGLs were imaged using an EVOS microscope cell-imaging system with an automated image collection protocol. The upper compartment was swabbed with a cotton swab to remove the non-migrated iMGLs. The remaining (migrated) iMGLs were imaged using the same microscope and automated image collection protocol. The total number of cells and number of

migrated cells were determined using an automated cell counting protocol with ImageJ. All analysis was performed using GraphPad Prism.

iMGL TREM2 Knockdown via Small-Interfering RNA (siRNA) (3.10)

50,000 iPSC-derived microglia-like cells were seeded per well in 96-well flat bottom tissue culture plates and matured for 7 days in 200 µL iMGL maturation media. Maturation media was comprised of: Advanced DMEM/F12, 1X PenStrep, 1X GlutaMax, 1X N2 Supplement, 55 µM BME, 10 ng/mL GM-CSF and 100 ng/mL IL-34. Over the 7 day maturation, media was replaced every 2 or 3 days. Upon completion of iMGL maturation, the maturation media was replaced with 200 µL maturation media and corresponding siRNA (either TREM2 siRNA or non-target siRNA) at 50 nM final concentration. Briefly, both the TREM2 and non-target siRNA were prepared as follows: stock siRNA was diluted 20X in Opti-Mem (Thermo #31985062). Next, stock Lipofectamine 3000 (Thermo #L3000015) was diluted 12.5X in Opti-Mem. Diluted siRNA and diluted Lipofectamine 3000 were combined in a 1:1 ratio, and then further diluted 5X in maturation media, resulting in the 50 nM final siRNA solution. At least 6 biological replicates were included for each condition. The iMGLs were incubated for 24 hours, then supernatants were frozen, and the remaining iMGLs were utilized for gene expression analysis.

RNA extraction and quantitative reverse transcription polymerase chain reaction (qRT-PCR) (3.11)

RNA was extracted from iMGL lysates with the RNeasy Micro Kit (Qiagen, Cat. No. 74004) following the manufacturer's protocol (excluding the optional on-column DNase digestion step). RNA concentration was measured on the Nanodrop ND-8000 following the manufacturer's protocol. Complementary DNA (cDNA) was derived from 200 ng total RNA using the Applied Biosystems High-Capacity cDNA Reverse Transcription (RT) kit (Applied Biosystems, Cat. No. 4374966) and was subjected to multiplexed specific target amplification (STA) using 2X TaqMan™ PreAmp Master Mix (Applied Biosystems, Cat. No. 4488593) and 20X TaqMan™ Gene Expression Assays (Applied Biosystems, see Supplemental Table 1 for list of

assays) following the protocol outlined in the Biomark X9 System Gene Expression and Genotyping User Guide (FLDM-01040 Rev 08). Preamplified cDNA was diluted 5X with 10 mM Tris, pH 8.0, 0.1 mM EDTA (TEKnova, Cat. No. T0221) and underwent qRT-PCR on the Biomark X9 System (Standard BioTools) following the 'Gene Expression Using the 96.96 IFC With TaqMan Assays' Express Probe GE workflow outlined in the FLDM-01040 Rev 08 User Guide. All qRT-PCR reactions were performed with six replicates for each of the samples. Cycle threshold (Ct) values were calculated using the Fluidigm Real-Time PCR Analysis software (v. 4.0.1) and exported. Relative expression of TREM2 in TREM2 siRNA-treated iMGLs was calculated for each sample using the 2-ΔΔCt ("delta-delta Ct") method in Excel. The delta Ct was calculated relative to the geometric mean of seven housekeeping genes (ACTB, B2M, GAPDH, GUSB, HPRT1, PPIA, XPO1) and the delta-delta Ct was calculated relative to the average delta Ct of the untreated WT cells. All figures were generated utilizing GraphPad Prism.

Participation in the Clinical Trials, and Collection of Cerebrospinal Fluid (CSF) (3.12)

Given the blinded nature of this analysis, the specific details of each clinical study will not be reported here. One hundred forty-eight (n=148) participants were enrolled in AD clinical trials, and CSF was collected from individuals with mild-cognitive impairment (MCI) or early AD. Two hundred twenty-one (n=221) participants were enrolled in ALS clinical trials, and CSF was collected from individuals with genetic and non-genetic (sporadic) forms of ALS. Seventy-six (n=76) participants were enrolled in PD clinical trials, and CSF was collected from individuals with genetic and non-genetic forms of PD. Sixty-four (n=64) participants were enrolled in PSP clinical trial, and CSF was collected from individuals with various forms of PSP.

Each clinical trial was conducted following Good Clinical Practice standards, and followed the Declaration of Helsinki and International Council for Harmonisation (ICH) requirements. Written informed consent was acquired by all individuals prior to initiating any study-related activities.

Olink® HT Explore Assay (Used for all CSF Testing) (3.13)

All human CSF samples were tested in partnership with Firalis, utilizing the Olink® Explore HT assay, following manufacturer's protocol. The Olink® Explore HT assay is a high-throughput assay that measures ~5400 proteins. A total of five hundred nine (n=509) CSF samples were analyzed. Initial data and quality control analyses were completed by Firalis. Additional analyses were performed internally, at Biogen. All data shown have been adjusted for age and sex of the study participants, and are presented as a geometric mean ratio (AD/disease) with significance values for each.

Results (Section 5)

TREM2 Cleavage into soluble TREM2 (sTREM2) is Impacted by Anti-TREM2 Antibody Mechanism of Action (5.1)

One of the most proximal effects of TREM2 activation is the cleavage into its alternate form, soluble TREM2 (sTREM2), whereby the production of sTREM2 subsequently terminates the TREM2 and DAP10/12 signaling pathway[19, 48]. Specifically, the TREM2 (and DAP10/12) signaling cascade is interrupted when the extracellular domain of TREM2 is shed (or cleaved) by A Disintegrin and metalloproteinase domain-containing protein 10 (ADAM10) or ADAM17, resulting in the production of sTREM2[48]. Previous studies have shown that both ligand and antibody binding of TREM2 increase sTREM2 levels[49, 50]. Although, in a separate study, researchers generated a TREM2 antibody that did not impact the cleavage of TREM2 into sTREM2[51]. Initially, we aimed to understand the effects of unique TREM2 activation on the production of sTREM2, using iPSC-derived microglia-like cells (iMGLs), which are a biologically relevant *in-vitro* model. These iMGLs have consistently been shown to express human microglia cell markers, such as IBA1 and PU.1 (internal – data not shown). As seen in the schematic of Figure 1, premature iMGLs (pMGLs) must be matured into iMGLs, prior to being treated with anti-TREM2 antibodies. Here, we wanted to see how the Alector and Vigil antibody impacted sTREM2 in iMGLs, particularly given the difference in binding properties and mechanisms of action for each antibody (Figure 2A). The Alector antibody binds the same site as ADAM10/17, which can simply be referred to as the stalk region of TREM2[52]. By binding this site, the Alector antibody acts as a shedding blocker, thus preventing the cleavage of TREM2 into sTREM2[52]. The Vigil antibody serves as a more pure TREM2 agonist, binding the IgV region of TREM2, thus making it more similar to some natural ligands of TREM2[41]. We utilized a soluble TREM2 (sTREM2) assay to demonstrate that the most proximal effects of TREM2 modulation are different between the two antibodies. As shown in Figure 2B, targeting TREM2 with the Alector antibody, which acts a shedding blocker, leads to a significant decrease

in sTREM2 in iMGL supernatant ($p<0.05$). Alternatively, the Vigil antibody, which serves as a more pure TREM2 agonist, leads to significantly increased sTREM2 (at 400 nM, $p<0.05$). These data provide initial evidence that differential targeting and activation of TREM2 leads to unique functional downstream effects.

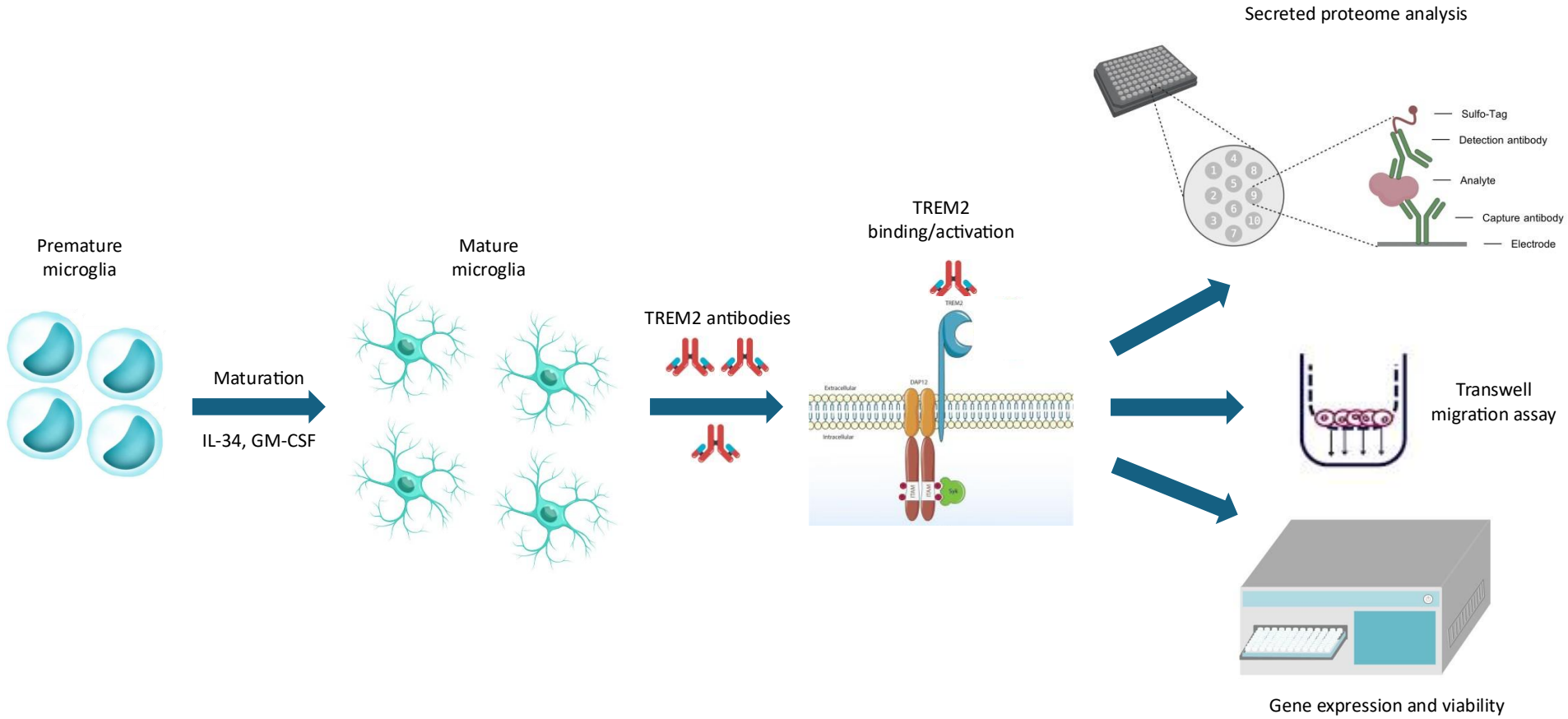

Figure 1. Schematic of the TREM2 modulation workflow with iPSC-derived microglia like cells (*also applicable to THP1-differentiated macrophages*)

Premature iMGLs (pMGLs) are matured for 7 days with media containing cytokine growth factors, IL-34 and GM-CSF. Following maturation, iMGLs are treated with anti-TREM2 monoclonal antibodies (24-72 hours) and following TREM2 activation, different functional assays are utilized. Functional outputs include secreted proteins (measured with MSD V-PLEX assays), migration (using transwell migraton) and viability (various Promega assays). *Note: for gene expression output, siRNA is used instead of anti-TREM2 antibodies.*

A

	Alector	Vigil
Isotype	hG1	hG1 aglycosylated
Effector function	Full	Low
Binding domain	Stalk, ADAM10/17 site	IgV
Mechanism	Shedding blocker, agonism through FcR binding	Agonism

B

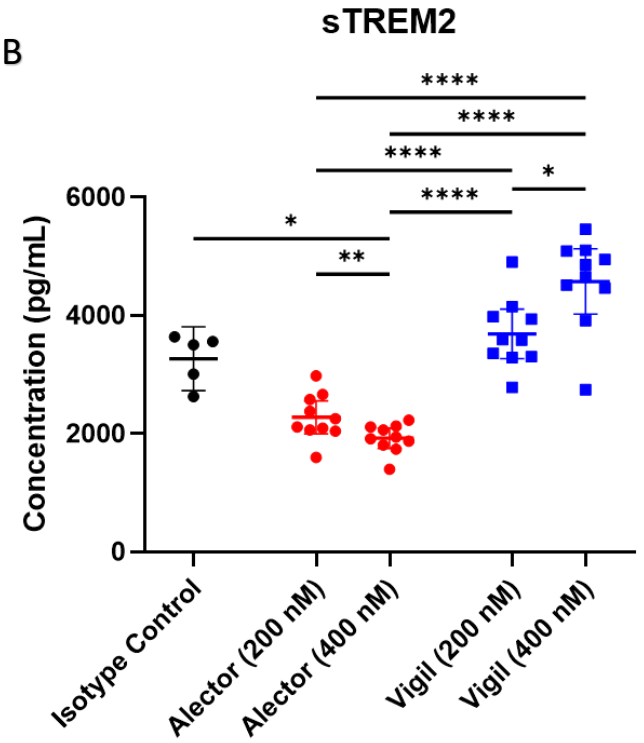

Figure 2. Soluble TREM2 (sTREM2) following TREM2 activation via two monoclonal antibodies with unique mechanisms of action.

Figure 2A – a table containing the properties of each anti-TREM2 monoclonal antibody. Figure 2B – a plot showing sTREM2 in iMGL supernatants (MSD S-PLEX assay) following treatment with each TREM2 antibody.

Note: * $p<0.05$, ** $p<0.01$, **** $p<0.0001$

IP-10 Release in THP1-derived macrophages (5.2)

Next, we used THP1-derived macrophages to investigate the effects of differential TREM2 binding. These immortal cells constitutively express TREM2, and are often used as an *in-vitro* model, given their homogenous nature when compared to more biologically relevant models. We investigated whether the two antibodies with different TREM2 binding capabilities had differential impacts on IP-10 secretion (MSD V-PLEX assay). Each antibody was tested in two conditions: complete maturation media (containing 10% FBS), and starved maturation media (excluding FBS). Previously, complete maturation media (containing 10% FBS) has been found to increase phosphorylated SYK (pSYK) in differentiated THP1s (*data not shown*). Since pSYK signaling is a direct result of TREM2 activation[19], this suggests that there is some baseline binding of TREM2 in differentiated THP1s when using media containing serum (10% FBS). In Figure 3A, the Alector antibody appears to increase IP-10 secretion in a dose dependent manner in THP1-derived macrophages following 24hr stimulation. In complete maturation media, there was a statistically significant increase in IP-10 concentration at 10 µg/mL Alector antibody, when compared to the control, 0 µg/mL antibody ($p<0.05$). In starved maturation media, there were no statistically significant increases in IP-10 concentration. Interestingly, when comparing complete and starved maturation media in the absence of any TREM2-targeting antibody, there's a clear difference in IP-10 concentration, furthering suggesting that serum can activate the TREM2 signaling pathway of differentiated THP1s. Ultimately, it's evident that the Alector antibody elevates the level of IP-10 in each assay condition, demonstrating that TREM2 activation alone with the Alector antibody results in IP-10 secretion. In Figure 3B, the Vigil antibody appears to increase IP-10 secretion as well, but the data do not suggest a dose-dependent effect. In complete maturation media, there was a statistically significant increase in IP-10 concentration at 15.0 µg/mL Vigil antibody, when compared to the control, 0 µg/mL antibody ($p<0.05$). In starved maturation media, there was a statistically significant increase in IP-10 concentration at 1.5 µg/mL ($p<0.05$). In these data as well, the difference in IP-10 secretion is clear

comparing the two media conditions. As such, these data suggest that TREM2 activation by the Vigil antibody alone results in in IP-10 secretion, which replicates earlier findings using the same antibody in human TREM2 transgenic mice[41].

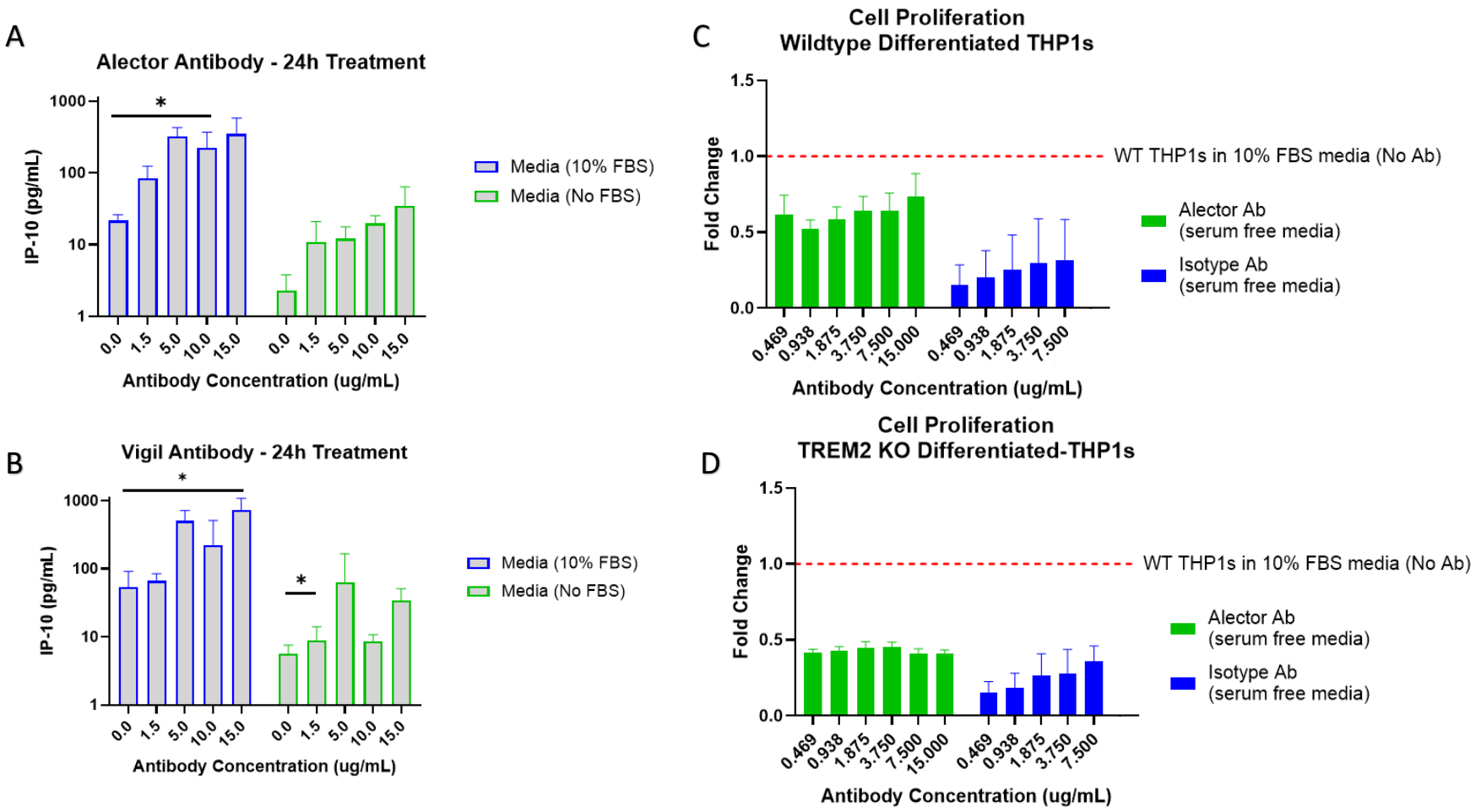

Figure 3. Monoclonal anti-TREM2 antibodies impact relevant functions in THP-1 derived macrophages.

Figure 3A – XY graph of IP-10 concentrations (MSD V-PLEX assay) in differentiated THP1 supernatant following 24-hour treatment with Alector antibody in two media conditions (+/- serum). Figure 3B - XY graph of IP-10 concentrations (MSD V-PLEX assay) in differentiated THP1 supernatant following 24-hour incubation/treatment with Vigil antibody in two media conditions (+/- serum). Figure 3C – XY graph of cell proliferation (CellTiter-Glo®) in wildtype differentiated THP1 lysates with Alector antibody treatment, as fold change versus wildtype control THP1-differentiated macrophages. Figure 3D – XY graph of cell proliferation (CellTiter-Glo®) in TREM2 knockout differentiated THP1 lysates with Alector antibody treatment, as fold change versus wildtype control THP1-differentiated macrophages. Note: * $p<0.05$

Viability of THP1-derived macrophages (5.3)

Wildtype (TREM2 expressing) THP1-derived macrophages have increased cell viability, as measured by CellTiter-Glo®, following treatment with the Alector antibody. CellTiter-Glo® is a commonly used assay, which measures the amount of adenosine triphosphate (ATP) following cell lysis. Quantifying ATP is a simple and clear indicator for the relative number of cells that are metabolically active, or viable. Modest increases in cell viability are seen at increasing antibody concentrations, whether using the Alector antibody or its isotype control (Figure 3C). Although, at each antibody concentration, there is a roughly 2-3 fold increase in viability when comparing the Alector antibody to the isotype control antibody. The data in Figure 3C suggest that there is a synergistic effect on cell viability when binding both TREM2 and Fc receptors simultaneously on THP1-derived macrophages.

TREM2 knockout (KO) THP1-derived macrophage viability is not impacted by the Alector antibody, no matter the concentration (Figure 3D). Interestingly, in these cells as well, it appears that increasing concentration of the isotype control antibody increases cell viability. These data further suggest that while TREM2 modulation alone increases the viability of THP1-derived macrophages, TREM2 and Fc receptor modulation have a synergistic impact on cell viability.

Both the wildtype and TREM2 KO data (Figures 3C and 3D) were generated in starved media conditions, as 10% FBS media has been previously shown to impact TREM2 signaling in THP1-derived macrophages (*data not shown*).

Development of a Transwell Migration Assay (5.4)

Human microglia can migrate to sites of injury[53], particularly to phagocytose damaging material, such as neurotoxic proteins and cell debris[32]. The data shown in Figure 4 highlight the ability for iPSC-derived microglia-like cells to migrate towards known chemoattractants[18, 54, 55], including Aβ1-42 fibrils and Complement 5a (C5a), although with a high degree of variability. In Figure 4B, for both Aβ1-42 fibrils and C5a, there is nearly a 2-fold range in the ratio of migrated cells. With such larger intra-assay variability, investigating the impacts of TREM2 modulation on migration is challenging. Nevertheless, following a 24h incubation with these ligands, iMGLs can successfully migrate through the 8.0 µm pores in the transwell migration assay format. In this experiment design, the iMGLs in the upper compartment (or on top of the transwell membrane) are placed in starved media (maturation media excluding GM-CSF and IL-34). The bottom compartments contain complete maturation media, as well as the chemoattractants. Given the pore size, it is possible for the chemoattractants (and cytokine growth factors, GM-CSF and IL-34) to move into the upper compartment. Yet, a concentration gradient is still established at the beginning of the incubation, allowing the iMGLs to sense and move towards these chemoattractants.

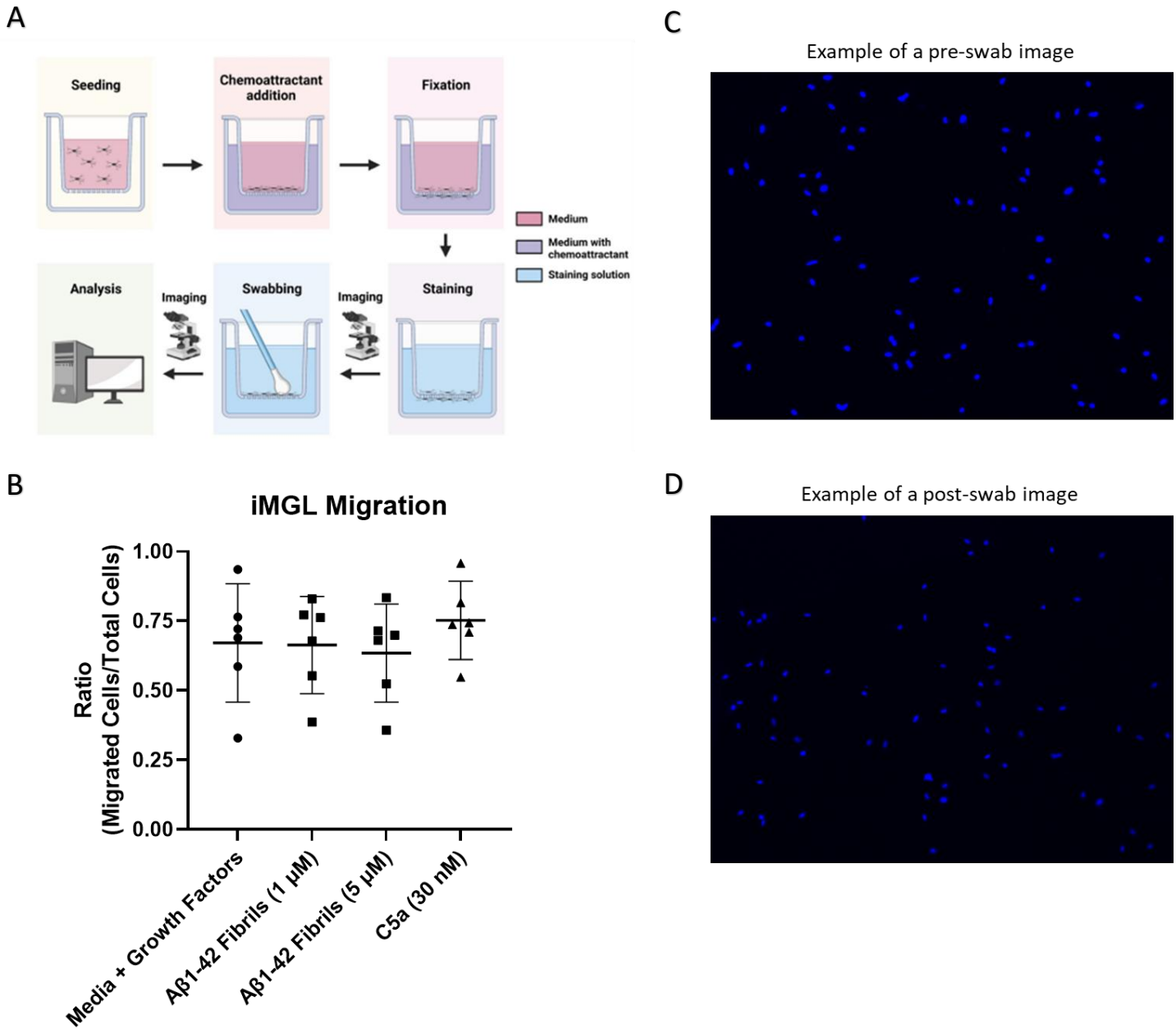

Figure 4. Development of an in-house transwell migration assay for iPSC-derived microglia-like cells (iMGLs)
Figure 4A – demonstrates the workflow of the transwell migration assay (schematic was adapted from Maguire et al[54]). Figure 4B – plot showing ratio of migrated cells/total cells using various chemoattractants. Figure 4C – an example of the image collected using an automated EVOS microscope before swabbing the upper membrane (total cells). Figure 4D – an example of the imaged collected using an automated EVOS microscope after swabbing the upper membrane (migrated cells only).

Chemokine Release in iMGLs following Vigil Antibody Treatment (5.5)

Next, we investigated whether the Vigil antibody had a dose-dependent impact on multiple chemokines and cytokines, using the MSD V-PLEX human chemokine and cytokine panel, respectively. These data are shown in Figure 5. The Vigil antibody caused measurable increases in 5 different chemokines, specifically IP-10, CCL2, CCL3, CCL4 and CCL13. When compared to control (400 nM antibody), each chemokine was significantly altered at multiple antibody concentrations. For IP-10, there was a significant decrease at 50 nM ($p<0.05$) and a significant increase at 200 nM ($p<0.0001$). For CCL2, there was a significant decrease at 50 nM ($p<0.001$) and significant increases at 200 nM and 400 nM ($p<0.0001$ and $p<0.001$, respectively). For CCL3, there were significant decreases at 50 nM, 100 nM and 400 nM ($p<0.05$, $p<0.05$, and $p<0.001$, respectively), while there was a significant increase at 200 nM ($p<0.001$). For CCL4, there was a significant increase at 200 nM ($p<0.001$). For CCL13, there were significant increases at 50 nM, 100 nM, 200 nM and 400 nM ($p<0.05$, $p<0.01$, $p<0.01$, and $p<0.0001$, respectively). Interestingly, four of the five chemokines reached peak secretion at 200 nM, prior to decreasing at 400 nM, likely demonstrating a hook-effect response with increasing antibody concentration. We hypothesize that this is likely due to reduced binding affinity once the antibody passes its saturation point. We believe at saturated concentrations of the Vigil antibody, it cannot effectively bind and cluster TREM2, due to individual antibody's competing for the same binding sites.

Notably, the remaining 5 chemokines and all cytokines (excluding GM-CSF as it's included in the iMGL maturation media) were all below the limit of quantitation (BLQ), prohibiting any conclusions to be drawn on the Vigil antibody's impact on these analytes.

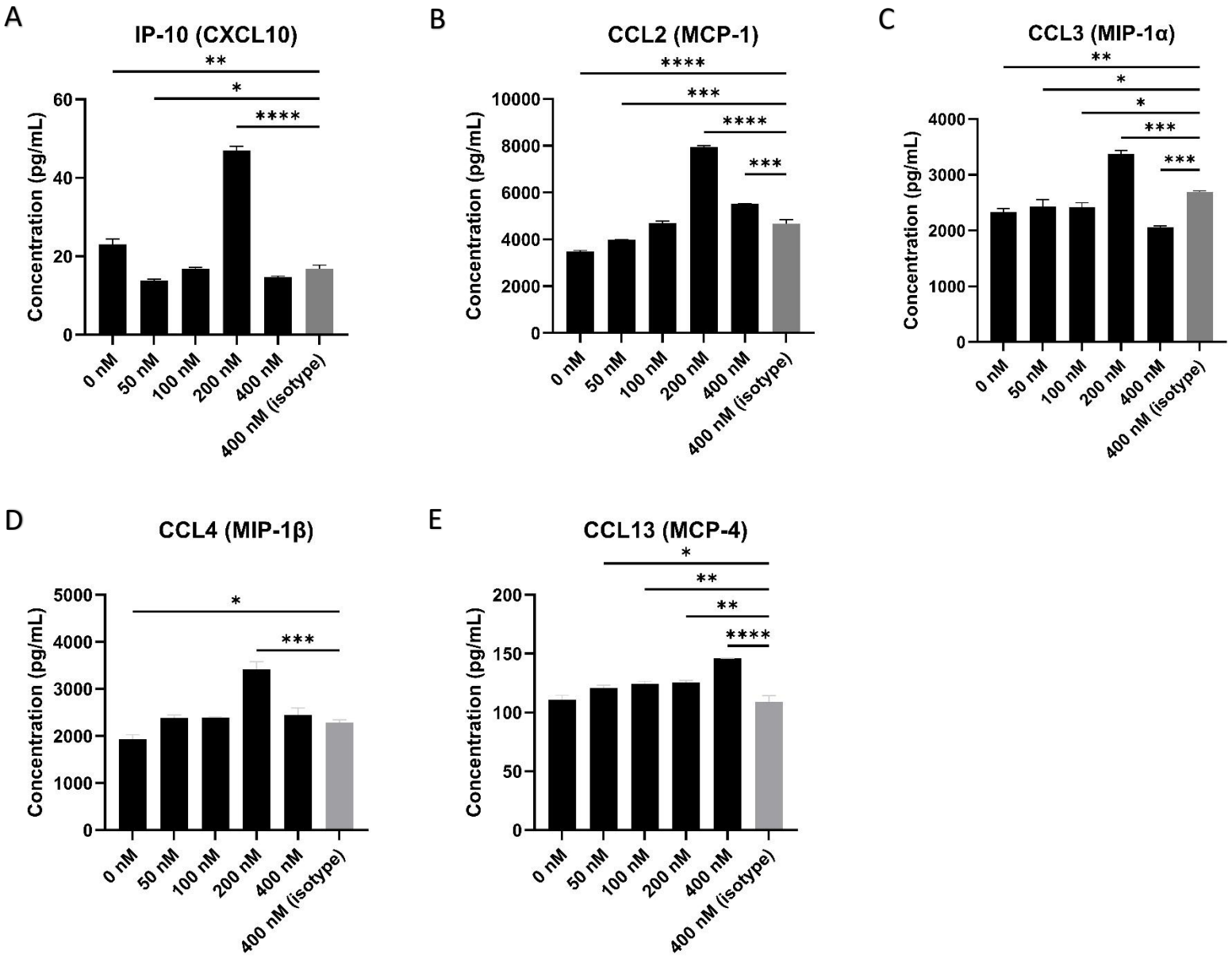

Figure 5. Vigil TREM2 antibody demonstrates hook-effect on chemokine secretions in iPSC-derived microglia-like cells (iMGLs)

Figure 5A-E – Measured protein concentration (MSD V-PLEX Human Chemokine Panel) in iMGL supernatants following incubation with Vigil antibody.

Note: * p<0.05, ** p<0.01, *** p<0.001, **** p<0.0001

Chemokine Release in iPSC-derived microglia-like cells (5.6)

To better understand the impacts of differential TREM2 activation on these iMGLs, we directly compared the Alector and Vigil antibody, as well as each of their isotype controls. These data are shown in Figure 6. We tested each antibody at 200 nM for 48h, subsequently measuring the chemokines with the same MSD V-PLEX chemokine panel. The Alector antibody significantly increased CCL4, CCL3 and CCL2 concentrations, when compared to its isotype control ($p<0.0001$ for each). The Vigil antibody significantly increased CCL4 and CCL2 concentrations ($p<0.0001$ for each), but had no significant impact on CCL3 secretion. Interestingly, when comparing the Alector and Vigil antibodies directly, the Alector antibody resulted in significantly higher levels of CCL4 and CCL3 ($p<0.0001$ for both), but significantly lower levels of CCL2 ($p<0.0001$). These findings are particularly interesting, as it suggests that the method of TREM2 activation differentially impacts downstream effects of chemokine secretion which could alter the neuroinflammatory state of these iMGLs and potentially, their surrounding environment. Notably, CCL2 is a chemokine with receptors on peripheral immune cells[56], and is implicated in the weakening of the blood-brain barrier (BBB) and subsequent recruitment of monocytes into the CNS[57].

In this *in-vitro* model, the Alector antibody and its isotype antibody had no difference on IP-10 secretion. While this does not replicate the earlier findings using differentiated THP1-derived macrophages, it's important to note the experiment designs were not identical. As such, it's important to further investigate the similarities and/or differences between the two *in-vitro* models. The Vigil antibody appears to increase the concentration of IP-10 when compared to its isotype control (and both Alector antibodies), but these data are not statistically significant.

The Alector antibody treatment resulted in significantly higher levels of CCL22, when compared its isotype control ($p<0.0001$). There was no difference between the Vigil antibody and its isotype. Interestingly, CCL22 secretion from the Alector antibody was also significantly higher than the Vigil antibodies ($p<0.0001$ for both).

Lastly, for CCL13, only the Vigil antibody significantly increased its concentration compared to isotype control ($p<0.05$). Additionally, the Vigil antibody was significantly higher than the Alector antibody ($p<0.01$). The receptor for CCL13 is found exclusively on peripheral immune cells[56], which provides further evidence that subtle differences in TREM2 activation could lead to vastly different downstream effects.

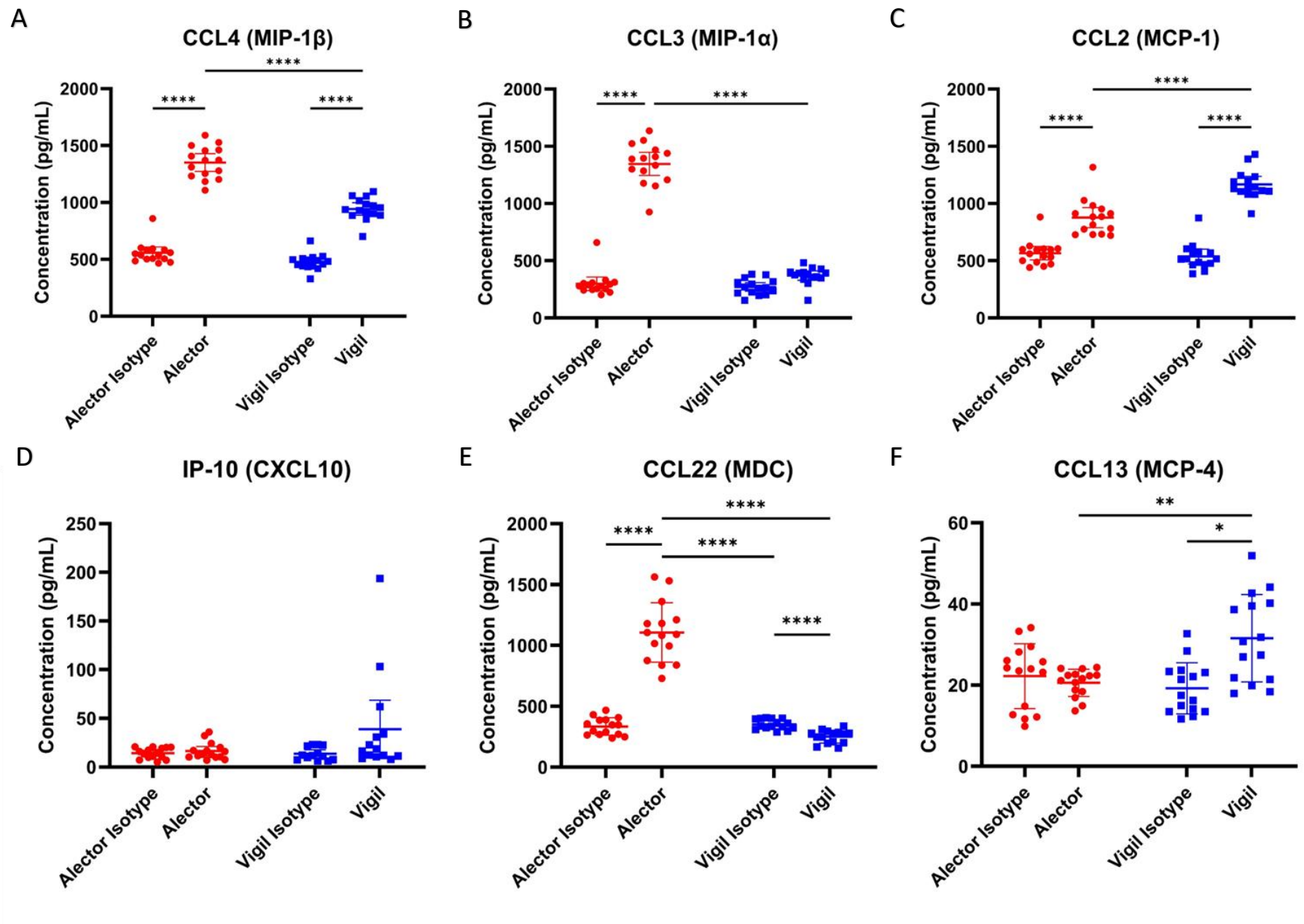

Figure 6. Alector and Vigil TREM2 antibodies have differing neuroinflammatory protein signatures following TREM2 modulation in iMGLs.

Figure 6A-F – Measured protein concentration (MSD V-PLEX Human Chemokine Panel) in iMGL supernatants following 48-hour antibody incubation (200 nM).

Note: * p<0.05, ** p<0.01, *** p<0.001, **** p<0.0001

iMGL Viability and Apoptosis Following Alector and Vigil Antibody Treatment (5.7)

Next, we aimed to better understand how TREM2 activation impacts the health of iMGLs by examining the impact of the TREM2-targeting antibodies on iMGL viability and apoptosis.

To measure the impact of both TREM2-targeting antibodies on cellular viability, iMGLs were treated with increasing concentrations of the Alector and Vigil antibodies, and viability was measured using a CellTiter-Glo® assay. While the Alector antibody, which blocks TREM2 receptor cleavage and increases receptor activity through FcR agonism, showed increased cellular viability (Fig. 7A), the Vigil antibody, which agonizes TREM2 receptor through IgV domain binding, demonstrated decreased cellular viability (Fig. 7B). These results are supported by an additional measurement of cellular viability using a CellTiter-Fluor™ assay (Fig. 7C). Here, a high dose of the Alector antibody induced increased cellular viability, while a high dose of the Vigil antibody induced slight decreases in cellular viability. Finally, a high dose of the Alector antibody reduced the levels of regulated cell death, while the Vigil antibody caused a slight increase in apoptosis (Fig. 7D), as measured by a Caspase Glo® 3/7 assay.

Overall, it appears that the Alector antibody has a more beneficial effect on iMGLs, specifically leading to an increase in viability and reduction in apoptosis. While the data for the Vigil antibody are not as striking, the data suggest a trend towards negative impacts on iMGL health. Ultimately, these data provide further evidence that the downstream effects of TREM2 activation can be meaningfully different depending on how TREM2 is engaged.

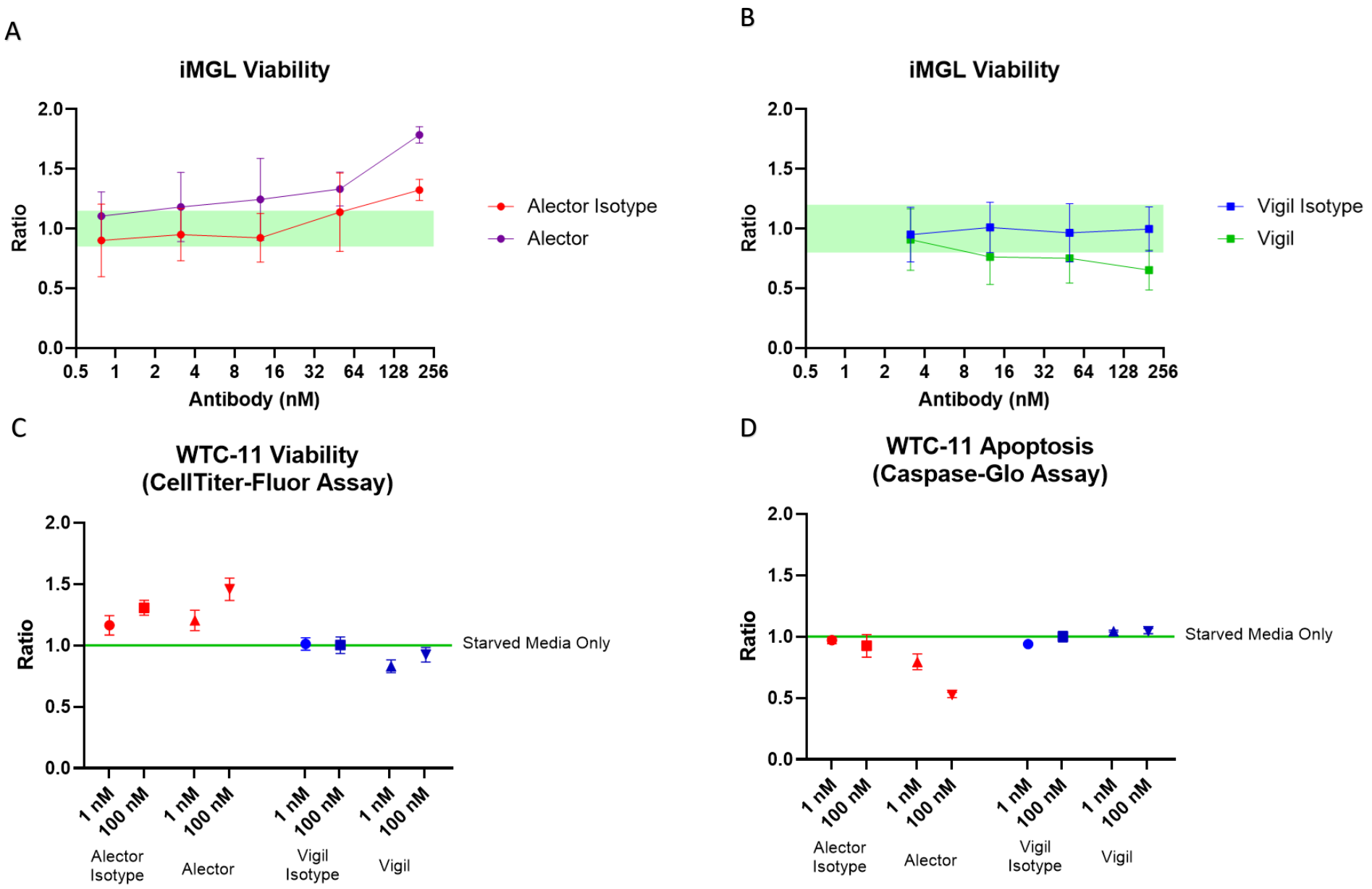

Figure 7. Impacts of TREM2 modulation on iMGL proliferation, viability, and apoptosis.

Figure 7A – XY graph of iMGL proliferation (CellTiter-Glo®) following Alector antibody treatment, as fold change vs. non-treated iMGLs. Figure 7B – XY graph of iMGL proliferation (CellTiter-Glo®) following Vigil antibody treatment, as fold change vs. non-treated iMGLs. Figure 7C – scatter plot of iMGL viability (CellTiter-Fluor™) following antibody treatment, as fold change vs. non-treated iMGLs. Figure 7D – scatter plot of iMGL apoptotis (Caspase-Glo® 3/7) following antibody treatment, as fold change vs. non-treated iMGLs.

TREM2 Knockdown in iPSC-derived microglia like cells (iMGLs) Utilizing Silencing RNA (siRNA) (5.8)

Next, we aimed to develop a method to reduce TREM2 gene expression in iMGLs, utilizing siRNA to understand the potential impacts of TREM2 downregulation on other functionally relevant genes expressed by microglia. Effective knockdown of TREM2 in iMGLs could be further utilized to study downstream functional effects, such as migration and viability. Here, and shown in Figure 8A, expression of TREM2 was significantly reduced by 87.7% relative to the wildtype control following incubation with 50 nM TREM2 siRNA for 24 hours ($p<0.0001$). While the non-target siRNA also significantly reduced TREM2 expression, the effect size was moderate (10.5%) when compared to the wildtype control ($p<0.01$). This is more likely due to biological and technical variability, as opposed to any specific TREM2 targeting. These data demonstrate an effective way to modulate TREM2 gene expression. Additionally, we have demonstrated internally that reduction of TREM2 gene expression results in the reduction of sTREM2 in iMGL supernatant *(data not shown*) following 48-hour and 96-hour incubation with the TREM2 siRNA. As such, this method of reduction in iMGLs is effective in specifically targeting TREM2.

We next evaluated what other genes were downregulated or upregulated following TREM2 siRNA exposure using qRT-PCR. As seen in Figure 8B, a reduction in TREM2 expression appears to increase IL-8 gene expression in these iMGLs by ~16 fold ($p<0.0001$). We hypothesize that TREM2 is required for optimal microglial viability and a reduction in TREM2 leads to a “stressed” state for iMGLs, resulting in the upregulation of IL-8 gene expression. However, given the effect size of the non-target siRNA on IL-8 (~6 fold increase, $p<0.0001$), these data also suggest that siRNA alone appears to impact the inflammatory response of iMGLs. Further evidence that siRNA alters the inflammatory state of iMGLs is shown in Figure 8C and 6D, where both CCL5 and IP-10 are significantly upregulated by non-target siRNA ($p<0.001$ and $p<0.0001$, respectively). While these genes are also significantly upregulated by the TREM2 siRNA, the small differences between target and non-target siRNA would suggest these increases are not TREM2 specific. We also evaluated other inflammation related genes, including IL-10, IL-6, IL-1β,

IL2RA, and IL-19, but none of these were impacted or their levels of expression were too low to quantify (data not shown).

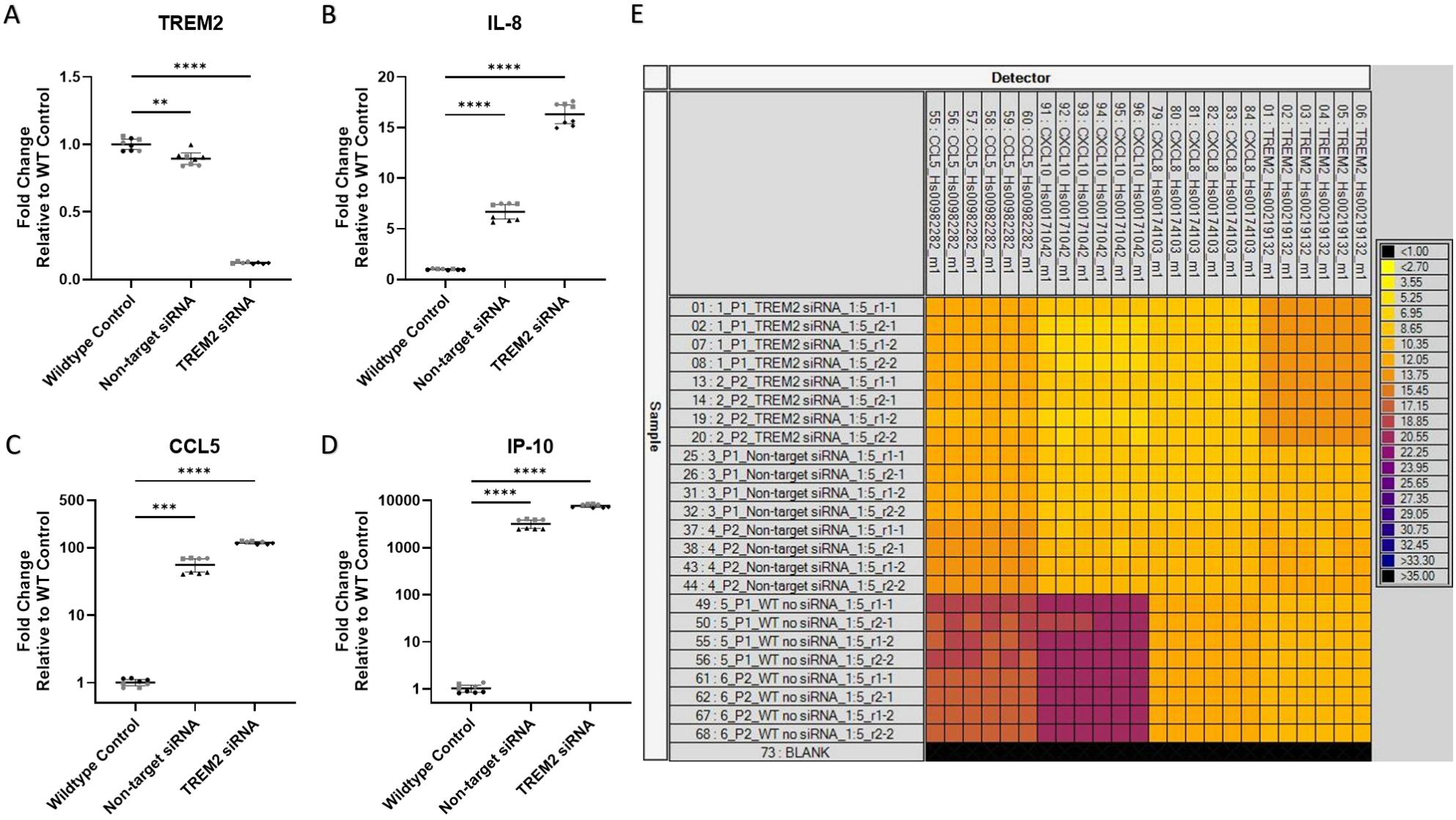

Figure 8. Effects of TREM2 siRNA on iPSC-derived microglia-like cell (iMGL) gene expression.

Figure 8A – TREM2 expression in iMGLs following 24h siRNA treatment (50nM). Figure 8B – IL-8 expression in iMGLs following 24h siRNA treatment (50nM). Figure 8C – CCL5 expression in iMGLs following 24h siRNA treatment (50nM). Figure 8D – IP-10 expression in iMGLs following 24h siRNA treatment (50nM). Figures 6A-D: black – biological replicates from plate 1, grey – biological replicates from plate 2. Figure 8E – heat map showing differences in gene expression amongst biological and technical replicates. Note: ** p<0.01, *** p<0.001, **** p<0.0001

Unique Expression of Proteins Associated with Microglial Function in AD CSF (5.9)

The Olink® HT Explore assay is a novel, high-throughput assay that can measure over 5400 proteins from a single sample, using as little as 2 µL of sample volume. The Olink® HT Explore is a proximity extension assay (PEA) that leverages next-generation sequencing (NGS) to measure relative protein concentrations in a given sample[58]. We tested 509 CSF samples using this technology and found hundreds of differentially expressed proteins in AD CSF, when comparing to other neurological diseases, specifically, ALS, PD and PSP. The number of CSF samples for each disease is as follows: 148 subjects with AD (MCI or early AD), 221 subjects with ALS (genetic and sporadic), 76 subjects with PD (genetic and non-genetic), and 64 subjects with PSP (various forms).

Specifically, we sought to identify proteins associated with microglial function that are elevated or decreased in AD CSF, when compared to at least one of the other neurological diseases. As shown in Supplemental Table 3, we found 22 proteins that are differentially expressed in AD CSF and related to microglial function. A few particularly interesting examples are highlighted in Table 2, including macrophage colony-stimulating factor 1 receptor (CSF1R), fractalkine (CX3CL1), integrin alpha-M (CD11b, or ITGAM), tyrosine-protein kinase Mer (MERTK), osteopontin (SPP1) and TREM2.

CSF1R, which we found to be elevated in AD CSF (compared to PSP CSF), is critical for microglial survival and viability, and inhibition of CSF1R leads to a robust depletion of microglia, both *in-vivo* and *in-vitro*[59-61]. Fractalkine, which we found to be increased in AD CSF (when compared to PSP CSF), is a chemokine expressed by neurons, and its receptor, CX3CR1 is expressed by microglia[62]. Fascinatingly, it has been suggested that the fractalkine/CX3CR1 interaction may both positively and negatively impact AD pathology depending on the stage of the disease[62]. CD11b, which is increased in AD CSF (compared to ALS, PD and PSP CSF), is a widely used and unique marker of microglia and is involved in microglial phagocytosis[63]. MERTK, which found elevated in AD CSF (compared to PSP CSF), is involved in many microglial functions, although is also frequently associated with microglial phagocytosis, specifically of

apoptotic cells and myelin debris[64]. Osteopontin, which is elevated in AD CSF (compared to PD CSF), but decreased in AD CSF (compared to PSP CSF), is expressed by numerous cells in the CNS, but has been specifically implicated in influencing microglial-dependent neuroinflammation[65]. Additionally, one recent study found that CSF osteopontin was strongly associated with other known CSF markers of AD pathology, including CSF Aβ42/40, CSF total tau and CSF phosphorylated tau181 (p-tau181)[66]. As such, osteopontin appears to be a potential biomarker with usefulness in both research and clinical settings. Lastly, TREM2 is clearly implicated in numerous essential microglial functions. Although, TREM2 expression alone is not likely to be as important to AD pathology, instead, whether the wildtype or a loss-of-function mutated form of TREM2 is expressed is what primarily influences AD pathology.

Overview of Differentially (and Significantly) Expressed Proteins in AD CSF (5.10)

After identifying specific proteins relevant for microglial function within AD CSF, we sought to understand more general differences between the diseased CSF samples. The data in Figure 9 illustrate the number of differentially expressed proteins between AD and each neurological disease. In comparison to ALS, there were 128 proteins with higher expression in AD CSF, and 54 proteins with lower expression in AD CSF. In comparison to PD, there were 69 proteins with higher expression in AD CSF, and 49 proteins with lower expression in AD CSF. Lastly, in comparison to PSP, there were 1089 proteins with higher expression in AD CSF, and 37 proteins with lower expression in AD CSF. Unsurprisingly, these data suggest a vast difference between AD CSF and each of the other neurological diseases. Some expected proteins are shown in the volcano plots in Figure 9, such as neurofilament light chain (NEFL), which is significantly higher in ALS CSF when compared to AD CSF. Another example is microtubule-associated protein tau (MAPT), or simply, tau, which is significantly higher in AD CSF, when compared to PSP CSF.

There were 39 proteins that were significantly different when comparing AD CSF to all 3 other neurological diseases. Most intriguingly, all 39 proteins are more highly expressed in the AD CSF samples. The five proteins that had the largest fold change (highest relative expression in AD CSF) included: tau, SHC-transforming protein 3 (Shc3), creatine kinase U-type (mitochondrial), CRACD-like protein and secreted frizzled-related protein 1 (SFRP1). The relative fold changes and adjusted p-values for these 5 proteins are listed in Table 1. Tau, as expected, was elevated in AD CSF, given it is the building block for neurofibrillary tangles of hyperphosphorylated tau (NFTs), which is one of the two main pathologies of AD. Shc3 is an interesting protein in this dataset, as a literature review suggests it has been less investigated in the context of AD. Shc3 is an adaptor protein (from the Shc family) that is typically expressed by neurons[67]. One study found that utilizing siRNA to reduce Shc3 expression *in-vitro*, led to a decrease in amyloid precursor protein (APP), Aβ42, and Aβ40[68]. Creatine kinase U-type,

mitochondrial is also known as ubiquitous mitochondrial creatine kinase (uMtCK), is a protein involved in energy metabolism[69] and has been found to interact with APP[70]. CRACD-like protein (or KIAA1211L) does not seem to have a known function, but was found to have lower brain tissue (frontal cortical tissue) expression in individuals with FTD-GRN (frontotemporal dementia due to mutations in the progranulin gene) than controls without dementia[71]. SFRP1 is a secreted protein and is associated with the Wnt signaling pathway[72], which interestingly, can also be activated by TREM2 signaling in microglia[73]. SFRP1 has also been suggested as link between ApoE4 and Aβ, such that when SFPR1 associates with ApoE4, it may lead to higher levels of Aβ production[74]. Overall, of the 5 proteins that are most highly expressed in AD CSF, there are markers that warrant further investigation to better understand their role in AD pathology. From the entire list of 39 proteins, there may also be proteins that could be further explored for clinical utility.

All 39 proteins that are differentially and significantly expressed in AD CSF are listed in Supplemental Table 2, including fold change and adjusted p-values.

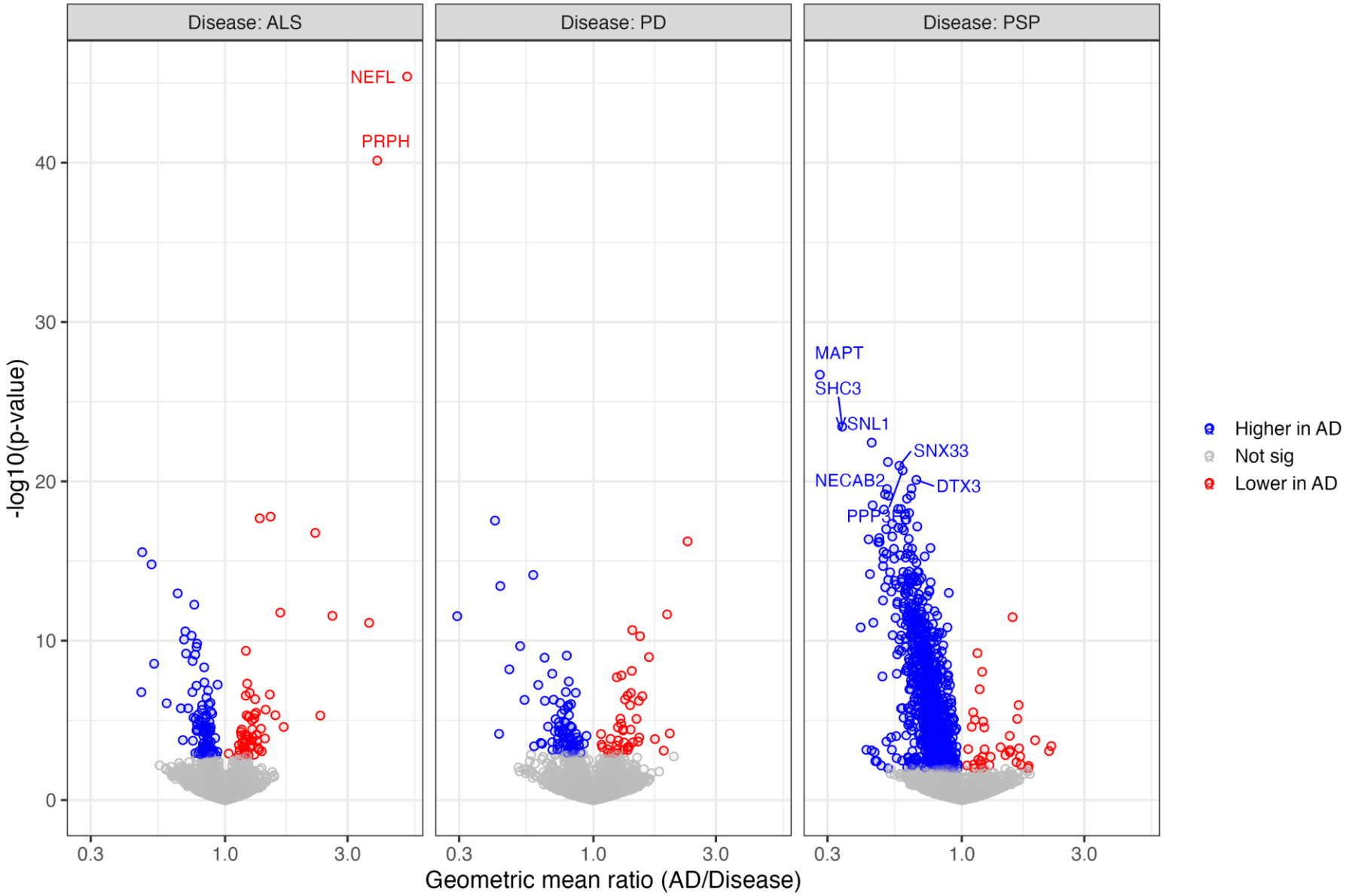

Figure 9. Volcano plots showing the differences in normalized protein expression (NPX) comparing AD CSF with ALS, PD and PSP CSF.
Blue dots demonstrate proteins with significantly higher NPX in AD CSF. Red dots demonstrate proteins with significantly lower NPX in AD CSF.
Grey dots show proteins without significant differences.

Table 1. Five most significantly increased proteins in Alzheimer's disease CSF.

Gene	Protein	ALS		PD		PSP	
		FC	adj_p	FC	adj_p	FC	adj_p
CKMT1A_CKMT1B	Creatine kinase U-type, mitochondrial	0.650	0.003827	0.538	0.000168	0.720	0.043218
CRACDL	CRACD-like protein	0.532	1.13E-05	0.481	1.41E-05	0.406	1.49E-09
MAPT	Microtubule-associated protein tau	0.481	4.02E-11	0.432	2.04E-10	0.282	8.6E-23
SFRP1	Secreted frizzled-related protein 1	0.661	0.000498	0.707	0.040592	0.441	3.04E-12
SHC3	SHC-transforming protein 3	0.524	4.05E-10	0.419	6.54E-13	0.345	2.26E-19

FC – fold change

Table 2. Proteins associated with microglial function in Alzheimer's disease CSF.

Gene	Protein	ALS		PD		PSP	
		FC	adj_p	FC	adj_p	FC	adj_p
CSF1R	Macrophage colony-stimulating factor 1 receptor	1.020	0.927247	1.078	0.633212	0.850	0.007071
CX3CL1	Fractalkine	0.988	0.974001	1.056	0.86243	0.817	0.005396
ITGAM	Integrin alpha-M	0.842	7.62E-05	0.799	8.75E-06	0.792	1.44E-07
MERTK	Tyrosine-protein kinase Mer	0.916	0.837281	0.902	0.889702	0.699	0.029659
SPP1	Osteopontin	1.001	0.993555	0.938	0.015944	1.056	0.011183
TREM2	Triggering receptor expressed on myeloid cells 2	1.056	0.862201	0.792	0.208047	0.643	1.95E-05

FC – fold change

Discussion (Section 6)

Alzheimer's disease is a devastating and debilitating neurodegenerative disease, defined by two main pathologies, Aβ plaques and neurofibrillary tangles of hyperphosphorylated tau (NFTs). Presently, there are limited treatment options available to slow the progression of the disease, all of which directly target Aβ pathology. In recent years, focus has increased on other pathologies that drive disease progression. One area in particular that has garnished much attention is neuroinflammation, which some now see as a driver of disease pathology, and not merely a consequence of AD progression[9]. Within the central nervous system (CNS), microglia, the resident immune cells, play a large role in brain homeostasis and can both protect from and contribute to neuroinflammation[25, 34]. TREM2 is a key receptor on microglia, and is involved in numerous microglial functions, including survival, migration, chemokine and cytokine release and phagocytosis[11]. Crucially, loss of function mutations in the TREM2 gene, particularly the R47H mutation, lead to an increased risk of developing Alzheimer's disease. Given its association with AD risk and key microglial functions, TREM2 has become an area of interest for therapeutic intervention. While there have been recent clinical setbacks for TREM2 candidates, many in the field are still interested in TREM2 as a therapeutic target. We aimed to investigate how TREM2 modulation impacts a few important microglial functions *in-vitro*, using two different, yet therapeutically relevant antibodies. The first, the Alector "mimic" antibody, activates the TREM2 (and DAP10/12) signaling cascade via simultaneous effector function. The second, the Vigil "mimic" antibody, is a more pure TREM2 agonist and has minimal, if any, effector function.

Initially, we opted to use THP1-differentiated macrophages to investigate the functional impacts of TREM2 modulation, as these cells are largely homogenous[75], constitutively express TREM2[43], and when differentiated, perform the same functions as microglia. In THP1-differentiated macrophages, we found increased IP-10 secretion following TREM2 activation with both monoclonal anti-TREM2

antibodies. IP-10 (or CXCL10) is a pro-inflammatory chemokine and binds the CXCR3 receptor, which is expressed on peripheral immune cells (T-cells and NK cells) and neurons in the CNS[56]. Interestingly, it has been reported that binding of IP-10 to neurons induces the extracellular signal-regulated kinases (ERK1/2) signaling cascade, which itself is involved in a number of cellular processes, including proliferation and survival, but also neuronal dysfunction and apoptosis[76-78]. The changes in the neuroinflammatory state that could be caused by IP-10 secretion, as a result of TREM2 signaling, may have both positive and detrimental effects on AD pathology, depending on the stage of disease. We also found that the Alector antibody increases cell viability in TREM2 expressing THP1-differentiated macrophages. Based on the differences between the Alector antibody and its isotype control, we hypothesize that the Alector binding and subsequent signaling pathway activation via TREM2 and Fc receptors may have a cumulative effect on these cells. Future experiments could utilize a modified Alector antibody with reduced (or eliminated) effector function to demonstrate whether there is any cumulative effect from binding TREM2 and Fc receptors.

Next, we focused on additional experiments using iPSC-derived microglia-like cells (iMGLs), as these are more biologically relevant cells and have greater similarity to human primary microglia. For the specific iMGLs we used in the study, we found that the cells were able to migrate towards known microglia chemoattractants[18, 54, 55], specifically Aβ1-42 fibrils and C5a, although with a high degree of variability. Migration is a key function of microglia, especially in the context of AD, as a response to Aβ and NFT pathology, where they can rapidly expand and retract their processes to move towards these proteins for degradation[79]. Given the variability in the transwell assay format, investigating the impacts of TREM2 modulation on migration was challenging. In future studies, the use of live cell imaging technologies (such as the IncuCyte) could reduce variability in the transwell migration assay, by allowing for more accurate cell counting and tracking. Alternatively, other migration assays could be considered, such as scratch/wound assays or microfluidic devices designed for migration. Ultimately, it would be

particularly insightful to utilize a migration assay with TREM2 antibodies and iMGLs with varying reductions in TREM2 (via siRNA) to determine if (or how) TREM2 activation can compensate for reduced TREM2 expression, which has been previously shown to impair migration[80].

To begin our assessment of different mechanisms of TREM2 activation impact microglial function, we utilized a soluble TREM2 (sTREM2) assay. We found that the Alector antibody led to a significant decrease in sTREM2, while the Vigil antibody led to a significant increase in sTREM2. Next, using two different multiplex MSD V-PLEX assays, we found differences in chemokine secretions from iMGLs depending on the antibody used to target TREM2. The Alector antibody and Vigil antibody generated varying patterns of chemokine secretions. Both antibodies significantly increased CCL4 and CCL2, albeit at different magnitudes. The Alector antibody significantly increased CCL3 and CCL22, while the Vigil antibody had no impact on CCL3 and significantly lowered CCL22. Lastly, the Alector antibody had no impact on CCL22, while the Vigil antibody significantly increased CCL22. Interestingly, neither antibody had an impact on IP-10 (unlike in THP1-differentiated macrophages). Taken together, these data may suggest that how TREM2 is modulated can lead to different inflammatory environments. Although, interpretation of these data about their possible connections to AD pathology should be taken with caution.

Using various cell health assays, we were able to demonstrate that the Alector antibody has a more beneficial effect on iMGL health, again suggesting that the ability to bind via TREM2 and Fc receptors leads to different effects. In fact, the Vigil antibody appeared to reduce overall cell health in the iMGLs. Although, with each *in-vitro* model, there are limits in the current dataset. In terms of proteome analysis, a relatively small set of proteins were analyzed (n=20 total cytokines and chemokines), which limited our understanding of how downstream protein secretions change with TREM2 activation. In the future, large scale proteomic analyses, such as unbiased mass spectrometry, or newer technologies, such as PEA-based immunoassay panels, could be used to understand broad protein changes. Viability could be

further assessed with live cell imaging technologies to have a more in-depth understanding of overall cell health during anti-TREM2 antibody treatments.

Utilizing the the Olink® HT Explore assay, we tested 509 CSF samples from various neurological diseases, including AD, ALS, PD and PSP. We identified hundreds of differentially expressed proteins in AD CSF, in comparison to the other neurological diseases. In comparing AD CSF to CSF from other neurological indications, there were more frequent instances of increased protein expression in AD CSF. Interestingly, we found 39 proteins that were significantly increased in AD CSF in comparison to all 3 other neurological diseases. The 5 proteins with highest AD CSF expression were tau, Shc3, uMtCK, CRACD-like protein, and SFRP1. Countless assays have been developed to measure numerous tau species in CSF, including total, pTau181 and MTBR-tau243[44, 45, 81, 82]. There are also blood-based tau assays, such as that for plasma pTau217[44, 45, 82]. Counterintuitively, most tau species assays actually better correlate with Aβ pathology[44, 45, 82], although there are many ongoing efforts in the field to identify and develop new assays targeting tau species that more accurately reflect tau pathology. Our data identified that tau protein is increased in AD CSF, which is widely understood in the field. However, additional novel analytes were also identified. From the other four proteins, SFRP1 likely warrants follow-up with a targeted assay in CSF, given that it is a secreted protein in the CNS[72]. Additionally, we identified 22 proteins that are differentially expressed in AD CSF and related to microglial function, including CSF1R, CX3CL1, CD11b, MERTK, osteopontin and TREM2. Of these, osteopontin is another interesting protein that should be considered in future studies with a targeted assay. Targeted assays would allow for absolute quantitation, and would enable more robust comparisons between each neurological disease. The profiling of AD CSF and other neurological disease CSF identified several differentially expressed proteins in AD CSF, although there are limitations with these data as well. The biggest limitation is the lack of a cognitively normal (CN) control group, which would be particularly useful in understanding the biological impact of these findings. Also, as previously mentioned, each

neurological disease is comprised of individuals with various subtypes of each disease. Additional analyses could be conducted to determine if there are any confounders within these subset populations, such as the genetic differences amongst each disease population. It could also help identify even more differences between AD CSF and the other diseases.

Conclusion (Section 7)

Overall, these *in-vitro* data suggest that there are differences in downstream signaling and impacts on microglial function depending on how TREM2 is targeted. Further investigation could include evaluation of the impacts on other microglial functions, as well as incorporating other therapeutically relevant TREM2 ligands, such as TREM2 targeting small molecules. Ultimately, these data give a small view into the wide-ranging effects of modulating TREM2.

The CSF profiling identified many differentially expressed proteins in Alzheimer's disease CSF, in comparison to ALS, PD and PSP CSF. Additional analyses are needed to understand how these differences may change amongst subgroups from each disease, and future studies should seek to include cognitively normal control groups. Ultimately, this wide range approach to measuring proteins in human CSF is particularly useful in identifying numerous potential targets of interest in precious samples.

Supplement Table 1 (Section 8.1) – List of qRT-PCR Assays

Gene	**Assay ID**
TREM2	Hs00219132_m1
ACTB	Hs99999903_m1
B2M	Hs99999907_m1
GAPDH	Hs02758991_g1
GUSB	Hs99999908_m1
HPRT1	Hs02800695_m1
PPIA	Hs99999904_m1
XPO1	Hs01034182_m1
IL10	Hs00961622_m1
IL6	Hs00174131_m1
IL1B	Hs01555410_m1
IL2RA	Hs00907779_m1
CCL5	Hs00982282_m1
CXCL8	Hs00174103_m1
CXCL10	Hs00171042_m1
IL18	Hs01038788_m1

Supplemental Table 2 (Section 8.2) - List of 39 proteins with differential expression in AD CSF (compared to all 3 other diseases).

Gene	Protein	ALS		PD		PSP	
		FC	adj_p	FC	adj_p	FC	adj_p
ACHE	Acetylcholinesterase	0.753	2.01E-08	0.823	0.007738	0.639	1.46E-15
ATP6V1G2	V-type proton ATPase subunit G 2	0.700	4.48E-07	0.797	0.039148	0.518	3.36E-17
CAP2	Adenylyl cyclase-associated protein 2	0.760	2.12E-08	0.799	0.000477	0.636	1.35E-16
CC2D1A	Coiled-coil and C2 domain-containing protein 1A	0.756	4.35E-08	0.822	0.007574	0.703	2.69E-10
CKMT1A_ CKMT1B	Creatine kinase U-type, mitochondrial	0.650	0.003827	0.538	0.000168	0.720	0.043218
CLEC5A	C-type lectin domain family 5 member A	0.762	0.003146	0.728	0.004479	0.776	0.007287
CRACDL	CRACD-like protein	0.532	1.13E-05	0.481	1.41E-05	0.406	1.49E-09
DDAH1	N(G),N(G)-dimethylarginine dimethylaminohydrolase 1	0.809	0.000786	0.816	0.015774	0.609	1.46E-15
DNAJA4	DnaJ homolog subfamily A member 4	0.814	0.003775	0.822	0.040752	0.624	1.56E-12
DNM1	Dynamin-1	0.814	0.005114	0.801	0.017443	0.651	3.19E-10
DTNB	Dystrobrevin beta	0.857	0.013807	0.824	0.007893	0.671	9.07E-13
DTX3	Probable E3 ubiquitin-protein ligase DTX3	0.828	3.93E-05	0.822	0.000509	0.665	2.08E-17
FABP3	Fatty acid-binding protein, heart	0.813	0.025229	0.769	0.014242	0.597	6.14E-11
GAP43	Neuromodulin	0.701	0.000196	0.730	0.015774	0.450	2.25E-16
HMOX2	Heme oxygenase 2	0.868	0.002835	0.872	0.031211	0.719	1.92E-13
HPCAL4	Hippocalcin-like protein 4	0.728	6.11E-07	0.777	0.004238	0.586	1.27E-14
ITGAM	Integrin alpha-M	0.842	7.62E-05	0.799	8.75E-06	0.792	1.44E-07
ITGB2	Integrin beta-2	0.846	0.015863	0.818	0.015774	0.783	0.000103
KIF5C	Kinesin heavy chain isoform 5C	0.837	5.55E-05	0.798	1.23E-05	0.736	1.76E-11
MAP2K1	Dual specificity mitogen-activated protein kinase kinase 1	0.882	0.000323	0.848	3.81E-05	0.802	2.66E-10
MAPT	Microtubule-associated protein tau	0.481	4.02E-11	0.432	2.04E-10	0.282	8.6E-23
MDH1	Malate dehydrogenase, cytoplasmic	0.828	0.002291	0.838	0.037175	0.669	7.28E-12
MMP10	Stromelysin-2	0.659	1.37E-08	0.596	1.15E-09	0.613	6.28E-10
NECAB1	N-terminal EF-hand calcium-binding protein 1	0.718	1.2E-05	0.762	0.009838	0.538	7.2E-15
NECAB2	N-terminal EF-hand calcium-binding protein 2	0.681	1.58E-08	0.692	1.25E-05	0.520	8.84E-18
PIGR	Polymeric immunoglobulin receptor	0.744	0.001196	0.724	0.004479	0.714	0.000227
PPP3R1	Calcineurin subunit B type 1	0.756	6.11E-07	0.834	0.036024	0.591	1.11E-17
RPH3A	Rabphilin-3A	0.670	1.98E-08	0.758	0.006129	0.518	1.02E-16
SCRN1	Secernin-1	0.830	0.020083	0.742	0.000268	0.566	4.65E-16
SDC4	Syndecan-4	0.857	0.000323	0.880	0.037976	0.774	1.85E-09
SFRP1	Secreted frizzled-related protein 1	0.661	0.000498	0.707	0.040592	0.441	3.04E-12
SH3PXD2B	SH3 and PX domain-containing protein 2B	0.836	0.001178	0.802	0.000493	0.702	2.77E-11
SHC3	SHC-transforming protein 3	0.524	4.05E-10	0.419	6.54E-13	0.345	2.26E-19
SNX33	Sorting nexin-33	0.728	3.86E-08	0.778	0.001101	0.574	8.84E-18
SOSTDC1	Sclerostin domain-containing protein 1	0.762	0.002179	0.656	8.75E-06	0.701	3.05E-05
STK32C	Serine/threonine-protein kinase 32C	0.793	0.002992	0.777	0.010002	0.791	0.002883
TMOD2	Tropomodulin-2	0.769	0.003392	0.708	0.000599	0.635	6.85E-08
TXNRD1	Thioredoxin reductase 1, cytoplasmic	0.855	0.000102	0.876	0.017547	0.757	9.59E-12
VSNL1	Visinin-like protein 1	0.766	0.004857	0.717	0.002669	0.448	7.49E-19

FC – fold change. In this table, fold changes closer to 0 mean greater expression in AD CSF.

Supplemental Table 3 (Section 8.3) - List of 22 proteins differentially expressed in AD CSF that are related to microglial function.

Gene	Protein	ALS		PD		PSP	
		FC	adj_p	FC	adj_p	FC	adj_p
AXL	Tyrosine-protein kinase receptor UFO	1.020	0.9144812	1.043	0.85553613	0.833	0.00034873
C1QA	Complement C1q subcomponent subunit A	0.993	0.9821116	1.061	0.7773666	0.808	0.0004202
C3	Complement C3	1.437	0.0010203	1.127	0.74451291	0.810	0.11621162
CD14	Monocyte differentiation antigen CD14	0.993	0.9867792	0.880	0.74058814	0.696	0.00250244
CD33	Myeloid cell surface antigen CD33	0.940	0.8385206	0.989	0.9903913	0.778	0.03418893
CSF1	Macrophage colony-stimulating factor 1	0.969	0.7773995	1.235	1.3515E-05	0.862	0.0008433
CSF1R	Macrophage colony-stimulating factor 1 receptor	1.020	0.9272466	1.078	0.63321191	0.850	0.00707139
CX3CL1	Fractalkine	0.988	0.9740005	1.056	0.86243009	0.817	0.00539588
GAS6	Growth arrest-specific protein 6	0.992	0.978876	1.050	0.84248961	0.819	0.00038943
GPNMB	Transmembrane glycoprotein NMB	1.254	0.0004982	1.111	0.48796428	0.999	0.9975943
IL34	Interleukin-34	0.932	0.634316	1.064	0.83112216	0.840	0.02306942
IL6ST	Interleukin-6 receptor subunit beta	0.939	0.4525865	1.024	0.92763122	0.765	2.6128E-09
ITGAM	Integrin alpha-M	0.842	7.625E-05	0.799	8.7538E-06	0.792	1.4361E-07
ITGB2	Integrin beta-2	0.846	0.0158626	0.818	0.01577442	0.783	0.00010346
LPL	Lipoprotein lipase	0.951	0.7747771	1.110	0.55078612	0.650	2.9686E-10
MERTK	Tyrosine-protein kinase Mer	0.916	0.8372807	0.902	0.88970212	0.699	0.02965894
PECAM1	Platelet endothelial cell adhesion molecule	0.979	0.9272466	0.975	0.94194804	0.791	9.2246E-05
SIGLEC10	Sialic acid-binding Ig-like lectin 10	1.101	0.3978479	1.064	0.81121885	0.836	0.01100427
SIGLEC8	Sialic acid-binding Ig-like lectin 8	1.179	0.0295059	0.975	0.95389001	0.869	0.06582598
SPP1	Osteopontin	1.001	0.9935552	0.938	0.01594363	1.056	0.01118339
TREM2	Triggering receptor expressed on myeloid cells 2	1.056	0.8622006	0.792	0.20804675	0.643	1.9489E-05
TYRO3	Tyrosine-protein kinase receptor TYRO3	0.949	0.5815743	1.015	0.96566281	0.796	5.9346E-07

FC – fold change. In this table, fold changes closer to 0 mean greater expression in AD CSF. Fold changes above 1 mean lower expression in AD CSF.

References (Section 9)

1. *Dementia vs. Alzheimer's Disease: What Is the Difference?* ; Available from: https://www.alz.org/alzheimers-dementia/difference-between-dementia-and-alzheimer-s.
2. *Dementia statistics*. Available from: https://www.alzint.org/about/dementia-facts-figures/dementia-statistics/.
3. *2024 Alzheimer's disease facts and figures.* Alzheimers Dement, 2024. **20**(5): p. 3708-3821.
4. DeTure, M.A. and D.W. Dickson, *The neuropathological diagnosis of Alzheimer's disease.* Mol Neurodegener, 2019. **14**(1): p. 32.
5. Ballard, C., et al., *Alzheimer's disease.* Lancet, 2011. **377**(9770): p. 1019-31.
6. Cummings, J., et al., *Lecanemab: Appropriate Use Recommendations.* J Prev Alzheimers Dis, 2023. **10**(3): p. 362-377.
7. Manly, J.J. and K.D. Deters, *Donanemab for Alzheimer Disease-Who Benefits and Who Is Harmed?* JAMA, 2023. **330**(6): p. 510-511.
8. Long, J.M. and D.M. Holtzman, *Alzheimer Disease: An Update on Pathobiology and Treatment Strategies.* Cell, 2019. **179**(2): p. 312-339.
9. Toader, C., et al., *Decoding Neurodegeneration: A Review of Molecular Mechanisms and Therapeutic Advances in Alzheimer's, Parkinson's, and ALS.* Int J Mol Sci, 2024. **25**(23).
10. Frost, J.L. and D.P. Schafer, *Microglia: Architects of the Developing Nervous System.* Trends Cell Biol, 2016. **26**(8): p. 587-597.
11. Bachiller, S., et al., *Microglia in Neurological Diseases: A Road Map to Brain-Disease Dependent-Inflammatory Response.* Front Cell Neurosci, 2018. **12**: p. 488.
12. Penney, J., et al., *iPSC-derived microglia carrying the TREM2 R47H/+ mutation are proinflammatory and promote synapse loss.* Glia, 2024. **72**(2): p. 452-469.
13. Lewcock, J.W., et al., *Emerging Microglia Biology Defines Novel Therapeutic Approaches for Alzheimer's Disease.* Neuron, 2020. **108**(5): p. 801-821.
14. Guerreiro, R., et al., *TREM2 variants in Alzheimer's disease.* N Engl J Med, 2013. **368**(2): p. 117-27.
15. Nguyen, A.T., et al., *APOE and TREM2 regulate amyloid-responsive microglia in Alzheimer's disease.* Acta Neuropathol, 2020. **140**(4): p. 477-493.
16. Raulin, A.C., et al., *ApoE in Alzheimer's disease: pathophysiology and therapeutic strategies.* Mol Neurodegener, 2022. **17**(1): p. 72.
17. Hunsberger, H.C., et al., *The role of APOE4 in Alzheimer's disease: strategies for future therapeutic interventions.* Neuronal Signal, 2019. **3**(2): p. NS20180203.
18. Hall-Roberts, H., et al., *TREM2 Alzheimer's variant R47H causes similar transcriptional dysregulation to knockout, yet only subtle functional phenotypes in human iPSC-derived macrophages.* Alzheimers Res Ther, 2020. **12**(1): p. 151.
19. Deczkowska, A., A. Weiner, and I. Amit, *The Physiology, Pathology, and Potential Therapeutic Applications of the TREM2 Signaling Pathway.* Cell, 2020. **181**(6): p. 1207-1217.
20. Hou, J., et al., *TREM2 dependent and independent functions of microglia in Alzheimer's disease.* Mol Neurodegener, 2022. **17**(1): p. 84.
21. da Silva Almeida, A., et al., *Building a potent TREM2 agonistic, biparatopic, common light chain antibody.* MAbs, 2025. **17**(1): p. 2546554.
22. Lessard, C.B., et al., *High-affinity interactions and signal transduction between Abeta oligomers and TREM2.* EMBO Mol Med, 2018. **10**(11).
23. Yeh, F.L., et al., *TREM2 Binds to Apolipoproteins, Including APOE and CLU/APOJ, and Thereby Facilitates Uptake of Amyloid-Beta by Microglia.* Neuron, 2016. **91**(2): p. 328-40.

24. Zhao, Y., et al., *TREM2 Is a Receptor for beta-Amyloid that Mediates Microglial Function.* Neuron, 2018. **97**(5): p. 1023-1031 e7.
25. Kober, D.L. and T.J. Brett, *TREM2-Ligand Interactions in Health and Disease.* J Mol Biol, 2017. **429**(11): p. 1607-1629.
26. Michael R. Daws, P.M.S., Erene C. Niemi, Thomas T. Chen, Nadia K. Tchao, and W.E. Seaman, *Pattern Recognition by TREM-2: Binding of Anionic*

Ligands1. The Journal of Immunology, 2003. **171**: p. 594-599.
27. Ulland, T.K., et al., *TREM2 Maintains Microglial Metabolic Fitness in Alzheimer's Disease.* Cell, 2017. **170**(4): p. 649-663 e13.
28. Yin, Z., et al., *Immune hyperreactivity of Abeta plaque-associated microglia in Alzheimer's disease.* Neurobiol Aging, 2017. **55**: p. 115-122.
29. Zhong, L., et al., *Soluble TREM2 induces inflammatory responses and enhances microglial survival.* J Exp Med, 2017. **214**(3): p. 597-607.
30. Wang, Y., et al., *TREM2 lipid sensing sustains the microglial response in an Alzheimer's disease model.* Cell, 2015. **160**(6): p. 1061-71.
31. Jay, T.R., et al., *TREM2 deficiency eliminates TREM2+ inflammatory macrophages and ameliorates pathology in Alzheimer's disease mouse models.* J Exp Med, 2015. **212**(3): p. 287-95.
32. Gao, C., et al., *Microglia in neurodegenerative diseases: mechanism and potential therapeutic targets.* Signal Transduct Target Ther, 2023. **8**(1): p. 359.
33. Millet, A., J.H. Ledo, and S.F. Tavazoie, *An exhausted-like microglial population accumulates in aged and APOE4 genotype Alzheimer's brains.* Immunity, 2024. **57**(1): p. 153-170 e6.
34. Paolicelli, R.C., et al., *Microglia states and nomenclature: A field at its crossroads.* Neuron, 2022. **110**(21): p. 3458-3483.
35. Kraller, M., et al., *Novel fully human high-affinity anti-TREM2 antibody shows efficacy in clinically relevant Alzheimer s mouse model.* Alzheimers Res Ther, 2025. **17**(1): p. 114.
36. Li, Y., et al., *TREM2: Potential therapeutic targeting of microglia for Alzheimer's disease.* Biomed Pharmacother, 2023. **165**: p. 115218.
37. Zgorzynska, E., *TREM2 in Alzheimer's disease: Structure, function, therapeutic prospects, and activation challenges.* Mol Cell Neurosci, 2024. **128**: p. 103917.
38. Colonna, M. and D.M. Holtzman, *Rethinking TREM2 as a target for Alzheimer's disease after the INVOKE-2 trial failure.* Nat Med, 2025. **31**(10): p. 3217-3218.
39. *Press Release: Sanofi to acquire Vigil Neuroscience, Inc., adding a new investigational medicine to treat Alzheimer's disease to the neurology pipeline*.
40. Wang, S., et al., *Anti-human TREM2 induces microglia proliferation and reduces pathology in an Alzheimer's disease model.* J Exp Med, 2020. **217**(9).
41. Larson, K.C., et al., *Rescue of in vitro models of CSF1R-related adult-onset leukodystrophy by iluzanebart: mechanisms and therapeutic implications of TREM2 agonism.* J Neuroinflammation, 2025. **22**(1): p. 26.
42. Fassler, M., et al., *Engagement of TREM2 by a novel monoclonal antibody induces activation of microglia and improves cognitive function in Alzheimer's disease models.* J Neuroinflammation, 2021. **18**(1): p. 19.
43. Korvatska, O., et al., *Triggering Receptor Expressed on Myeloid Cell 2 R47H Exacerbates Immune Response in Alzheimer's Disease Brain.* Front Immunol, 2020. **11**: p. 559342.
44. Hansson, O., *Biomarkers for neurodegenerative diseases.* Nat Med, 2021. **27**(6): p. 954-963.
45. Zetterberg, H. and K. Blennow, *Moving fluid biomarkers for Alzheimer's disease from research tools to routine clinical diagnostics.* Mol Neurodegener, 2021. **16**(1): p. 10.

46. Tijms, B.M., et al., *Cerebrospinal fluid proteomics in patients with Alzheimer's disease reveals five molecular subtypes with distinct genetic risk profiles.* Nat Aging, 2024. **4**(1): p. 33-47.
47. Haenseler, W., et al., *A Highly Efficient Human Pluripotent Stem Cell Microglia Model Displays a Neuronal-Co-culture-Specific Expression Profile and Inflammatory Response.* Stem Cell Reports, 2017. **8**(6): p. 1727-1742.
48. Steiner, A., et al., *gamma-Secretase cleavage of the Alzheimer risk factor TREM2 is determined by its intrinsic structural dynamics.* EMBO J, 2020. **39**(20): p. e104247.
49. Filipello, F., et al., *Soluble TREM2: Innocent bystander or active player in neurological diseases?* Neurobiol Dis, 2022. **165**: p. 105630.
50. Schlepckow, K., et al., *Enhancing protective microglial activities with a dual function TREM2 antibody to the stalk region.* EMBO Mol Med, 2020. **12**(4): p. e11227.
51. Zhao, P., et al., *Discovery and engineering of an anti-TREM2 antibody to promote amyloid plaque clearance by microglia in 5XFAD mice.* MAbs, 2022. **14**(1): p. 2107971.
52. Long, H., et al., *Preclinical and first-in-human evaluation of AL002, a novel TREM2 agonistic antibody for Alzheimer's disease.* Alzheimers Res Ther, 2024. **16**(1): p. 235.
53. Tieu, T., et al., *Physiological and injury-induced microglial dynamics across the lifespan.* Cell Rep, 2025. **44**(7): p. 115991.
54. Maguire, E., et al., *Assaying Microglia Functions In Vitro.* Cells, 2022. **11**(21).
55. Ryu, J.K., et al., *Microglial VEGF receptor response is an integral chemotactic component in Alzheimer's disease pathology.* J Neurosci, 2009. **29**(1): p. 3-13.
56. Wojcieszak, J., K. Kuczynska, and J.B. Zawilska, *Role of Chemokines in the Development and Progression of Alzheimer's Disease.* J Mol Neurosci, 2022. **72**(9): p. 1929-1951.
57. Westin, K., et al., *CCL2 is associated with a faster rate of cognitive decline during early stages of Alzheimer's disease.* PLoS One, 2012. **7**(1): p. e30525.
58. Wik, L., et al., *Proximity Extension Assay in Combination with Next-Generation Sequencing for High-throughput Proteome-wide Analysis.* Mol Cell Proteomics, 2021. **20**: p. 100168.
59. Elmore, M.R., et al., *Colony-stimulating factor 1 receptor signaling is necessary for microglia viability, unmasking a microglia progenitor cell in the adult brain.* Neuron, 2014. **82**(2): p. 380-97.
60. Hu, B., et al., *Insights Into the Role of CSF1R in the Central Nervous System and Neurological Disorders.* Front Aging Neurosci, 2021. **13**: p. 789834.
61. Spangenberg, E., et al., *Sustained microglial depletion with CSF1R inhibitor impairs parenchymal plaque development in an Alzheimer's disease model.* Nat Commun, 2019. **10**(1): p. 3758.
62. Pawelec, P., et al., *The Impact of the CX3CL1/CX3CR1 Axis in Neurological Disorders.* Cells, 2020. **9**(10).
63. Hopperton, K.E., et al., *Markers of microglia in post-mortem brain samples from patients with Alzheimer's disease: a systematic review.* Mol Psychiatry, 2018. **23**(2): p. 177-198.
64. Nguyen, L.T., et al., *Mertk-expressing microglia influence oligodendrogenesis and myelin modelling in the CNS.* J Neuroinflammation, 2023. **20**(1): p. 253.
65. Rosmus, D.D., et al., *The Role of Osteopontin in Microglia Biology: Current Concepts and Future Perspectives.* Biomedicines, 2022. **10**(4).
66. Quesnel, M.J., et al., *Osteopontin: A novel marker of pre-symptomatic sporadic Alzheimer's disease.* Alzheimers Dement, 2024. **20**(9): p. 6008-6031.
67. Magrassi, L., et al., *Shc3 affects human high-grade astrocytomas survival.* Oncogene, 2005. **24**(33): p. 5198-206.
68. Xie, Z., et al., *RNA interference silencing of the adaptor molecules ShcC and Fe65 differentially affect amyloid precursor protein processing and Abeta generation.* J Biol Chem, 2007. **282**(7): p. 4318-4325.

69. Burklen, T.S., et al., *The creatine kinase/creatine connection to Alzheimer's disease: CK-inactivation, APP-CK complexes and focal creatine deposits.* J Biomed Biotechnol, 2006. **2006**(3): p. 35936.
70. Li, X., et al., *Stabilization of ubiquitous mitochondrial creatine kinase preprotein by APP family proteins.* Mol Cell Neurosci, 2006. **31**(2): p. 263-72.
71. Miedema, S.S.M., et al., *Distinct cell type-specific protein signatures in GRN and MAPT genetic subtypes of frontotemporal dementia.* Acta Neuropathol Commun, 2022. **10**(1): p. 100.
72. Wu, W., et al., *Secreted frizzled-related proteins in angiogenesis: molecular mechanisms and clinical implications.* Angiogenesis, 2025. **29**(1): p. 12.
73. Zheng, H., et al., *TREM2 Promotes Microglial Survival by Activating Wnt/beta-Catenin Pathway.* J Neurosci, 2017. **37**(7): p. 1772-1784.
74. Oveisgharan, S., et al., *Proteins linking APOE varepsilon4 with Alzheimer's disease.* Alzheimers Dement, 2024. **20**(7): p. 4499-4511.
75. Ahmed, A., P. Rozario, and Y. Zhu, *Differentiation and Polarization of THP-1 Cells into M1 and M2 Macrophages for Cancer Research.* Methods Mol Biol, 2026. **2983**: p. 205-213.
76. McKimmie, C. and D. Michlmayr, *Role of CXCL10 in central nervous system inflammation.* International Journal of Interferon, Cytokine and Mediator Research, 2014.
77. Meng Qi Xia M.D., P.D., Brian J. Bacskai Ph.D., Roger B. Knowles Ph.D., Shi Xin Qin M.D., Ph.D., Bradley T. Hyman M.D., Ph.D., *Expression of the chemokine receptor CXCR3 on neurons and the elevated expression of its ligand IP-10 in reactive astrocytes: in vitro ERK1/2 activation and role in Alzheimer's disease.* Journal of Neuroimmunology, 2000. **108**(1-2): p. 227-235.
78. Wortzel, I. and R. Seger, *The ERK Cascade: Distinct Functions within Various Subcellular Organelles.* Genes Cancer, 2011. **2**(3): p. 195-209.
79. Lee, C.Y. and G.E. Landreth, *The role of microglia in amyloid clearance from the AD brain.* J Neural Transm (Vienna), 2010. **117**(8): p. 949-60.
80. Mazaheri, F., et al., *TREM2 deficiency impairs chemotaxis and microglial responses to neuronal injury.* EMBO Rep, 2017. **18**(7): p. 1186-1198.
81. Horie, K., et al., *CSF MTBR-tau243 is a specific biomarker of tau tangle pathology in Alzheimer's disease.* Nat Med, 2023. **29**(8): p. 1954-1963.
82. Blennow, K. and H. Zetterberg, *Biomarkers for Alzheimer's disease: current status and prospects for the future.* J Intern Med, 2018. **284**(6): p. 643-663.